(2)

# Icing Prevention by Ultrasonic Nucleation of Supercooled Water Droplets in Front of Subsonic Aircraft



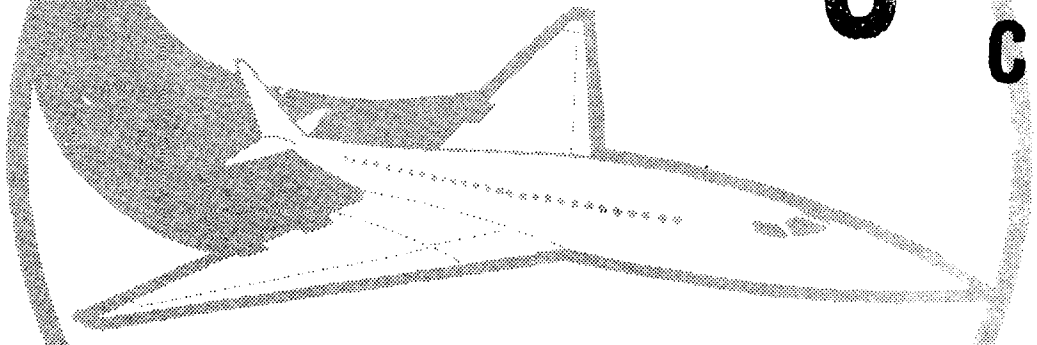

October 1992

DOT/FAA/CT-TN92/38



U.S. Department of Transportation
Federal Aviation Administration

Technical Center
Atlantic City International Airport, N.J. 08405

NOTICE

This document is disseminated under the sponsorship of the U. S. Department of Transportation in the interest of information exchange. The United States Government assumes no liability for the contents or use thereof.

The United States Government does not endorse products or manufacturers. Trade or manufacturers' names appear herein solely because they are considered essential to the objective of this report.

**Technical Report Documentation Page**

| 1. Report No. | 2. Government Accession No. | 3. Recipient's Catalog No. |
|---|---|---|
| DOT/FAA/CT-TN92/38 | | |

| 4. Title and Subtitle | 5. Report Date |
|---|---|
| ICING PREVENTION BY ULTRASONIC NUCLEATION OF SUPERCOOLED WATER DROPLETS IN FRONT OF SUBSONIC AIRCRAFT | September 1992 |
| | 6. Performing Organization Code |
| 7. Author(s) | 8. Performing Organization Report No. |
| Douglas R. Worsnop, Richard Miake-Lye, and Ze'ev Hed | DOT/FAA/CT-TN92/38 |
| 9. Performing Organization Name and Address | 10. Work Unit No. (TRAIS) |
| Aerodyne Research, Inc.<br>45 Manning Road<br>Billerica, MA 01821 | 11. Contract or Grant No.<br>DTFA03-91-C-00038 |
| | 13. Type of Report and Period Covered |
| 12. Sponsoring Agency Name and Address | Technical Note |
| U.S. Department of Transportation<br>Federal Aviation Administration<br>Technical Center<br>Atlantic City International Airport, NJ 08405 | 14. Sponsoring Agency Code<br>ACD-230 |

15. Supplementary Notes

COTR: Carmen F. Munafo, FAA Technical Center

16. Abstract

Experiments were performed in the NASA Lewis Research Center (LeRC) Icing Research Tunnel (IRT) to explore the possible application of a novel icing prevention technique. This technique is based on nucleation ice crystallization in supercooled cloud droplets upstream of the impingement surface and relying on evaporative cooling to remove the latent heat of fusion from the droplet so that it can completely freeze before striking the solid surface. Ice accretion on the impingement surface was measured to quantify the changes due to induced nucleation.

A flow duct was designed to provide a uniform, parallel flow from the nucleation excitation volume to the test surface, a simple symmetric airfoil. The distance between the excitation volume and the airfoil in the flow duct could be varied, but the maximum length of over 2 meters (m) was chosen to maximize the time for freezing. Ice accretion was measured over a range of tunnel parameters, including tunnel velocities of 50-100 miles per hour (mph) and temperatures from 0 to -36 °F. At colder temperatures, spontaneous freezing of supercooled droplets led to reductions in observed ice accretion. However, the range of active nucleation parameters explored in this set of experiments had no measurable effect on ice accretion on the subject airfoil. Suggested future work includes expanding the measurement parameter space and obtaining static measurements in a cloud chamber.

| 17. Key Words | 18. Distribution Statement |
|---|---|
| Aircraft Icing<br>Ice Protection<br>Ice Nucleation<br>Ice Crystallization | Document is on file at the Technical Center Library, Atlantic City International Airport, New Jersey 08405 |

| 19. Security Classif. (of this report) | 20. Security Classif. (of this page) | 21. No. of Pages | 22. Price |
|---|---|---|---|
| Unclassified | Unclassified | 57 | |

## PREFACE

This project is an outgrowth of a previous FAA sponsored SBIR contract (DTRS-57-90-00132). Continued research was feasible due to the additional FAA funding and the support of NASA LeRC Icing Research Tunnel (IRT) personnel. Beyond making the wind tunnel available, their logistical and system support was crucial for the experimental testing described in this report.

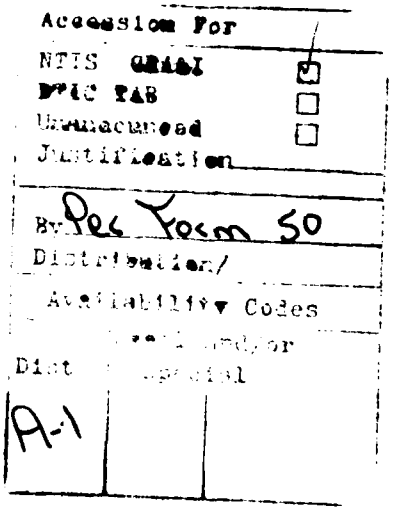

TABLE OF CONTENTS

## LIST OF ILLUSTRATIONS

## LIST OF TABLES

## EXECUTIVE SUMMARY

Experiments were performed to explore the possible application of a novel icing prevention technique in NASA Lewis Research Center's (LeRC) icing research flow facility, the Icing Research Tunnel (IRT). This technique is based on nucleating ice crystallization in the supercooled cloud droplets using ultrasonic acoustic radiation. Acoustic energy in the range of 10 to 650 kilohertz (kHz) was produced with a combination of piezoelectric ceramic single-frequency transducers and broad-band high performance loudspeakers (tweeters with extended range to 40 kHz).

The ultrasonic energy excites a volume in the IRT droplet-laden airflow upstream of a subject impingement surface, a streamlined-tubing airfoil, to perturb liquid droplets and initiate the freezing nucleation process. Between the excitation volume and impingement on the subject airfoil, evaporative cooling was expected to remove the latent heat of fusion from the droplet so that it could freeze before striking the solid surface. The distance separating these two points was chosen based on estimates of the heat removal rates. Ice accretion on the impingement surface was measured to quantify the changes due to induced nucleation.

A flow duct was designed at Aerodyne Research, Inc. (ARI) and built by NASA LeRC to provide a uniform, parallel flow from the nucleation excitation volume to the test surface. A 30.5- by 61.0-centimeter (cm) (1- by 2-foot) duct, 244 cm (8 feet) long, was aligned with the flow near the center of the IRT test section. The duct samples the most uniform region of the IRT flow and directs it toward the subject airfoil, preventing mixing or residual flow angularity from perturbing the flow path. Thus the flow volume, excited by the ultrasonic radiation upstream of the airfoil in the flow duct, is convected along the duct (with minimal mixing at its edges) before impinging on the airfoil.

The distance in the flow duct between the excitation volume and the airfoil could be varied by attaching the transducer mounting plate at one of three positions along the duct's wall. The maximum length of over 2 meters was chosen in the reported experiments to maximize the time for freezing. The IRT velocity was kept near the minimum, 22 meters per second (50 miles per hour), at which reliable droplet sizes and flow and droplet uniformity could be maintained. For a given transducer/airfoil separation, the lowest flow velocity maximizes the freezing time for the excited droplets. Experiments were performed with two different droplet size distributions and liquid water content in the flow. Tunnel temperatures ranging from -18 °C to -39 °C (0 °F to -36 °F) were used with a variety of ultrasonic excitation parameters for each temperature.

Ice accretion was measured along the 61-cm span of the airfoil over 10 minutes of ice accumulation time in the tunnel. At cold, <-34 °C (<-30 °F), temperatures, reduced ice accretion was consistent with homogeneous freezing (and non-accretion) of ice particles. However, for the range of excitation parameters explored in this set of experiments, no significant effects on ice accretion on the subject airfoil due to ultrasonic excitation were observed. Future work is suggested for expanding the measurement parameter space in order to more fully understand the previously reported anecdotal evidence for

such acoustically-induced freezing. The proposed extensions to the current work include increasing the ultrasonic power densities beyond the high levels (125 decibel (dB)) used in the reported experiments and possibly performing non-flowing measurements in a static, supercooled cloud chamber.

# 1. TECHNICAL BACKGROUND

## 1.1 Introduction

The ultimate goal of this research program is to determine the feasibility of a new aircraft anti-icing technique, based on projection of ultrasonic acoustic energy in front of aircraft. Acoustic perturbation would induce freezing of supercooled cloud droplets in front of the aircraft so that frozen ice particles will bounce rather than accrete on aircraft surfaces. The specific goal of this research reported here was to demonstrate ultrasonically-induced nucleation in front of an airfoil surface.

This work was preceded by a laboratory study of ultrasonic freezing of droplets supercooled in a low pressure vacuum system. Based on that work, which was unsuccessful, ARI proposed to test the concept at realistic, atmospheric pressure, using a suitably equipped wind tunnel to simulate icing conditions. A schematic of the proposed test is shown in figure 1.

The tests were carried out in the NASA LeRC Icing Research Tunnel (IRT). Building on experience gained from previous FAA Small Business Innovative Research (SBIR) support, Aerodyne personnel designed and constructed an assembly containing a total of nine acoustic transducers and associated drive electronics. In conjunction with NASA LeRC personnel, a test flow duct was assembled in the IRT and interfaced with the transducer assembly.

During the period of 15-19 December 1991, supercooled droplets generated in the IRT were irradiated with ultrasonic energy over a range of conditions. Droplet freezing was monitored by measuring ice accretion on an airfoil mounted at the end of the test duct. The background and implications of the failure to reduce observed ice accretion are the focus of this report.

In the remainder of Section 1, the technical background of ice nucleation in general and of ultrasonically induced nucleation in particular are given. This is followed by a discussion of the time required for droplet freezing. These considerations formed the basis for the test design and research plan.

In Section 2, the test apparatus and procedure are described. Section 3 reports the results of actual test measurements. Finally, in Section 4, the results and their implications are discussed. Section 5 gives conclusions.

## 1.2 Aircraft Deicing

Currently, ice protection for general aviation aircraft is provided either by thermal means (heating elements or hot medium circulation), by mechanical means (inflatable rubber boots), or sometimes by transpiration bleeding of melting point suppressants

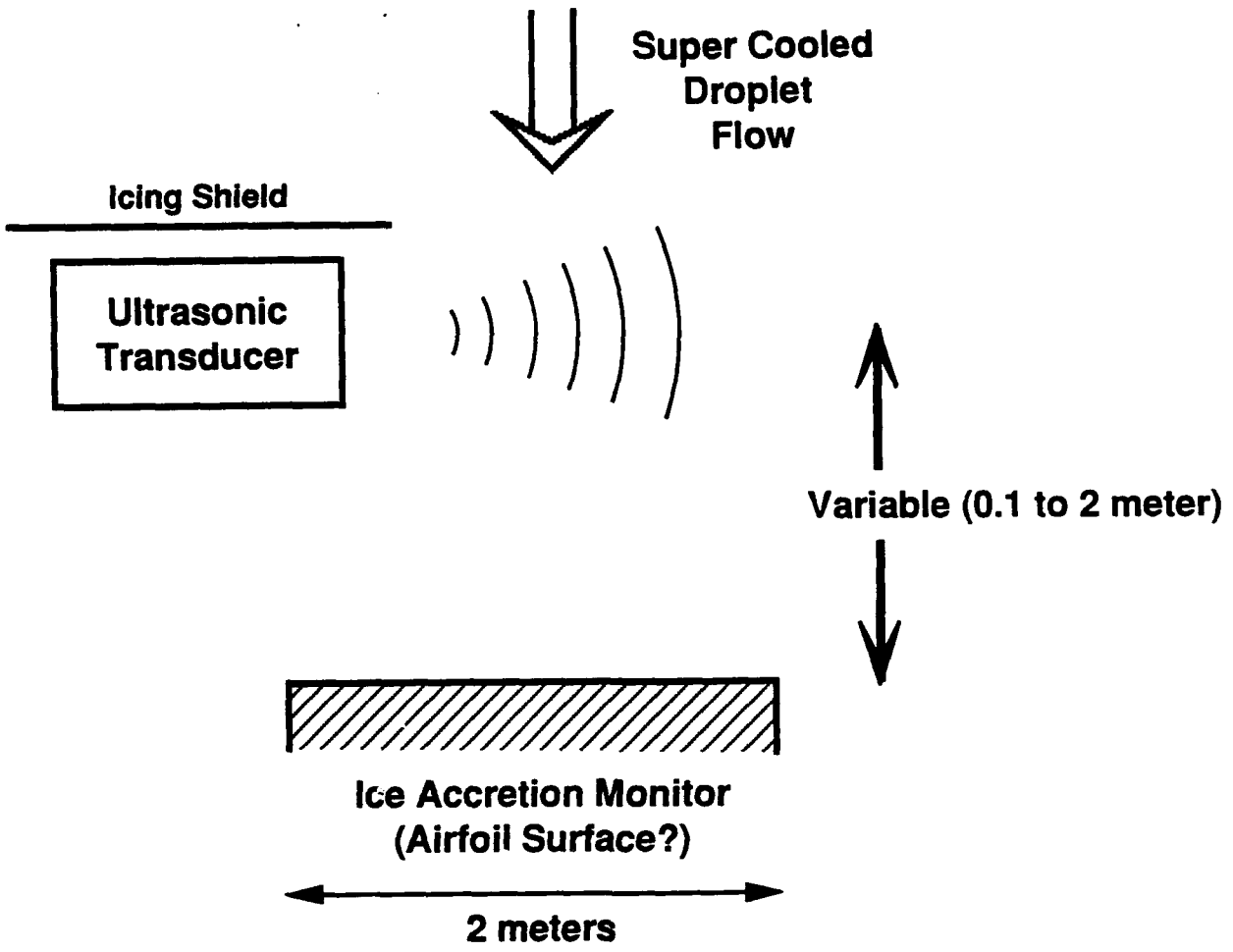


Figure 1. SCHEMATIC OF ULTRASONIC ICE NUCLEATION TEST
Ultrasonic transducers irradiate transversely across wind tunnel flow of supercooled droplets. Ice accretion is monitored on a surface placed downstream of the transducers. Measurement of accretion thickness as a function of distance from the transducer will map out kinetics of the nucleation/freezing processes.

on the leading edges (glycol based deicing systems). These systems are either bulky, have finite flight time capabilities or consume large amounts of energy. A new anti-icing strategy involving ice nucleation and freezing of the supercooled water droplets prior to their impingement and solidification on the leading edges of the wings and fuselage of the aircraft was proposed. Application of this approach would induce cavitation nucleation or perturbation nucleation in the supercooled droplets by ultrasound emitted from a series of transducers implanted in the leading edges or the fuselage.

If the ultrasonic energy can be delivered efficiently, then the approach will broaden the operational capabilities of general

aviation aircraft by decreasing the weight and the energy consumption relative to current systems. The goal of this project was to determine the basic physical parameters underlying the ultrasonic nucleation process in order to assess the potential for actual implementation of ultrasonic anti-icing.

## 1.3 Ice Nucleation

The process by which a liquid crystallizes when cooled below its melting point involves two distinct mechanisms, crystal nucleation and crystal growth. The driving force for freezing is the difference in free energy between the liquid and solid phases at a given temperature (primarily determined by the heat of fusion).

The condition for the triggering of the phase transition between the liquid and the solid phases is the formation of embryonic nuclei in the liquid. This requires the establishment of surfaces between the liquid and the newly formed nuclei, which requires energy to perturb the liquid. Since the surface energy of each embryonic nucleus increases with the square of its radius (surface area) and the difference in free energy between its solid state and its liquid state increases with the cube of its radius (volume), one can see that very small nuclei are not stable since the surface energy of the nucleus is larger than the energy gained from fusing its volume.

Once a critical size of such an embryonic nucleus has been reached, however, the energy gained from the heat of fusion is larger than the energy required to increase the nucleus' surface, and thus their further growth lowers the free energy of the system. Such nuclei are therefore thermodynamically favored; they are stable and continue to grow until the liquid phase is converted to the crystalline phase. The minimal radius of a stable embryonic nucleus is termed the critical radius, and is the radius at which the gain in free energy between the two states equals the energy required to form the new surface.

Differences between homogeneous and heterogeneous nucleation in solidifying liquids are noted. Homogeneous nucleation rates depend only on the thermodynamic properties of the liquid in question. Heterogeneous nucleation occurs on pre-existing surfaces (usually undissolved impurities or external solid surfaces). The presence of such surfaces removes the need to supply the energy for forming the embryonic nucleus' surface, or, at least, dramatically reduces the surface formation energy, and thus the critical radius.

For any liquid, in principle, a homogeneous solidification temperature can be defined, which would be the lowest possible (equilibrium) temperature at which super-cooled liquid can exist. Due to the impossibility of maintaining systems absolutely free of any impurities, there are always some uncertainties in the determination of this temperature. For water, however, a temperature of -40°F is well accepted as the homogeneous freezing

temperature.[1] Freezing of water at temperatures higher than the homogeneous freezing temperature requires the presence of pre-existing nucleating surfaces.

Icing conditions in the atmosphere are created when water droplets cool below 32°F in the absence of any nucleating agents. When an aircraft enters a cloud formation containing supercooled water droplets, the solid surfaces of the leading edge serve as nucleation sites for the supercooled droplets, and icing occurs. While this is a simplistic explanation of a more complex phenomenon, it is well known that icing does not occur at very low temperatures where the droplets have undergone homogeneous nucleation and only ice particles are present. It is surmised, therefore, that if nucleation and freezing in advance of their impingement on the aircraft can be effected, then the ice particles will bounce from the aircraft structure and ice accretion will be avoided.

In the atmosphere super-cooled droplets often (if not usually) freeze heterogeneously on solid impurities (e.g. dust or soot particles) within the droplet. Heterogeneous nucleation of supercooled droplets has been induced with silver iodide crystals, and the heterogeneous nucleation temperature can be raised as high as -7°F.[2] An alternative nucleating agent is the naturally occurring micro-organism pseudomonas syringae, capable of raising the heterogeneous nucleating temperature to the range of -5 to -9°F.[3] It is not practical, however, to use these techniques for the purpose of avoiding icing in flight. Delivery of nuclei in front of a moving plane would be cumbersome, the weight penalty too large and, moreover, the environmental impact of such an approach could be problematic.

### 1.4 Ultrasonically Induced Nucleation

Therefore, the investigation of an alternative mode of heterogeneous nucleation was proposed, whereby the lowering of the surface energy is provided by ultrasonic induced density fluctuations within the droplets (or on their surfaces). The technique, also known as cavitation nucleation, has been used successfully in the solidification of larger masses. There is anecdotal evidence of such effects for aerosols, though there has not been any systematic study of the phenomenon. For example, major rain discharges from clouds with laden supercooled droplets are known sometimes to occur immediately following a lightning stroke (and its accompanying thunder). One can speculate that sudden acoustic pressure waves could cause nucleation and thus agglomeration of supercooled droplets. While the same energy density in a system of airborne transducers is impractical, it could be possible that fine tuning would result in a similar localized effect at much lower energy densities.

Reports of more direct anecdotal observations appeared in 1941. Ronald L. Ives[4] reported that, under some circumstances, noise disturbances (mostly in the audible range) of high intensity and with a broad spectral distribution, were capable of enhancing droplet nucleation and coalescence in "River Fogs" (supercooled mountain cap clouds). However, the mechanisms for the observed behavior were never elucidated and the reproducibility of the experiments was ambiguous. Nevertheless, some indication of a non-vanishing interaction between acoustic energy and supercooled droplets was evident.

The Ives report prompted a comment by Swinbank,[5] who reported that during WW II that the British Meteorological Office had tested ultrasonic anti-icing in a wind tunnel, with negative results. In fact, they observed enhanced ice accretion, which they interpreted as evidence of partial freezing of the supercooled droplets. This is actually evidence of a positive ultrasonic nucleation effect, since, as discussed below, ice crystal nucleation and liquid droplet freezing are physically separate processes. No details of the wind tunnel testing were reported; thus, it is not possible to quantify the significance of their observations. Thus, this observation must be considered anecdotal and its explanation speculative, though physically reasonable, i.e. partially frozen droplets may indeed have enhance accretion efficiencies.

During the course of this project, a patent issued in 1949 for "Method of Crystallizing Super-Cooled Water Droplets"[6] was discovered. Originally directed toward fog reduction at airports, the authors did note the potential for aircraft anti-icing applications. The patent referred to laboratory observations of siren-induced freezing of supercooled droplets in a cloud chamber. A copy of the patent is included as Appendix A. The patent reports that audible and ultrasonic frequencies up to 30 kHz were effective in causing nucleation and that power levels of 150 dB were required. The principal author, Florence van Straten of Bethesda, MD, was contacted and she confirmed the experimental results, but indicated that the laboratory results were never formally reported. Again the details reported in the patent are insufficient to evaluate potential application to aircraft anti-icing. In particular, there is no indication of the origin of the 150 dB nucleation threshold nor of the frequency range of the acoustic output of the siren.

The van Straten patent points out the two key parameters that need to be evaluated for understanding of ultrasonically induced ice nucleation: acoustic frequency range and minimum energy density. Both are key to specifying electrical power and mechanical transducer requirements for eventual airborne anti-icing application. This project was designed to provide the first systematic study of ice nucleation effects induced by a wide range of acoustic frequencies.

Based on these anecdotal observations, the test plan included utilization of acoustic frequencies ranging from the audible to the ultrasonic. Transducers in the audible (and near audible) range are readily available as high performance audio 'tweeter' components, which give continuous frequency coverage in the range 1 to 40 KHz. Ultrasonic frequencies (up to 1 MHz) require specification of piezoelectric transducers at fixed, resonant frequencies. Three such transducers were specified at 80, 350 and 650 KHz. Power levels were maximized within the limits of available transducers and their associated electrical amplifier/drivers.

In the proposal initiating this study, power requirements derived from first principles were estimated. This discussion is included as Appendix B. The estimate involved comparing the energetics of formation of requisite embryonic ice nuclei with available acoustic energy densities. The latter involves the intrinsic problem of large mismatches in acoustic impedances in the transducer/air/droplet system. These mismatches occur between the transmitting medium (air) on one side and the transducer's outer surface and the water droplets on the sending and receiving sides, respectively. The estimated minimum power requirements are not inconsistent with the 150 dB levels reported in the van Straten patent. However, because of assumptions required for these calculations, there is considerable uncertainty in their accuracy and applicability, hence the need for empirical measurements.

These calculations emphasize the need for minimizing the mismatch in transducer/air acoustic impedance. Building on previous FAA supported work,[7] ultrasonic transducers with 35-40 dB losses at the air interface (as compared to 80 dB losses for conventional designs) were specified and procured. As reported in Section 2, the capability to generate audible and ultrasonic acoustic waves at power levels of up to ~125 dB resulted.

The research plan was to test ultrasonically induced ice nucleation by irradiating a wind tunnel flow of supercooled water droplets with the acoustic transducers described above. Such nucleation would be monitored by measuring ice accretion on an airfoil surface downstream of the transducers. However, the relationship between ice particle nucleation and subsequent accretion of ice on a surface depends on the freezing of the liquid droplet in the intervening time.

## 1.5 Droplet Freezing

Freezing of the entire volume of a super-cooled water droplet is a physically separate process from the initial nucleation of a single ice crystal within the droplet. The nucleation process, as discussed above, is essentially a molecular process, involving the formation of small embryonic nuclei whose volume is very small relative to that of a cloud droplet. Once nucleation has been initiated, the freezing of the volume of the entire droplet must be

considered separately. In the context of anti-icing in flight, the question is: How far in the front of the aircraft must ice nucleation be initiated?

The rate of freezing needs to be compared to aircraft speed and the distance in front of leading edge surfaces. As a reference point, consider a distance of one meter which, at 400 mph, corresponds to ≈ $5 \times 10^{-3}$ seconds (s). This is very long compared to most molecular processes, i.e. there is no fundamental, physical process limiting water droplet freezing on this millisecond scale. In fact, in previous work at Aerodyne it has been shown that super-cooled droplets can indeed freeze into "snow" in less than $10^{-3}$ s.[8]

On a millisecond time scale the rate of freezing is actually a heat transfer problem. Upon ice nucleation, liquid freezes until release of latent heat of fusion warms the droplet to the freezing point, 32°F. At that point, more liquid can freeze only as heat of fusion (80 cal/g) is removed to maintain the temperature at 32°F. By far the most efficient heat removal process is evaporation of water molecules, since the heat of vaporization of water (600 cal/g) is so much larger than the heat of fusion. In previous laboratory work at Aerodyne,[8] molecular collision limited evaporation at low pressure (<3 torr) allowed very fast freezing (< $10^{-3}$ s).

At atmospheric pressure, evaporative cooling will be limited by gas-phase diffusion of water vapor away from the droplet. The driving force for water vapor evaporation is proportional to the difference between the liquid water vapor pressure at 32°F (e.g. 4.5 torr) and the ambient water vapor pressure (at the super-cooled droplet temperature). The rate of gas diffusion of water vapor away from the droplet is inversely dependent on the droplet volume and the rate of cooling for the entire droplet is directly dependent on the droplet surface area.

The overall rate of the above processes is estimated below. The diffusion limited evaporation rate is given by[9]

$$R_E = \frac{\Delta n \ \gamma_g \ c \ \pi d^2}{4} \ \text{(mole/s)}$$

where the rate of diffusion is expressed as the collision probability coefficient

$$\gamma_g = \frac{8 \ D_g}{c \ d}$$

where $\Delta n = n_{32°F} - n_T$ subscript denotes temperature
$n$ = vapor density (mole/cm$^3$)
$c$ = mean molecular speed (cm/s)
$D_g$ = gas diffusion coefficient (cm$^2$/s)
$d$ = droplet diameter (cm)

The rate of heat removal from the droplet is given by the product of $R_E$ and the heat of vaporization of water $C_V$

$$R_H = R_E \, C_V \, \frac{18 \text{g/mole}}{6 \cdot 10^{23} \text{ mol/mole}} \quad \text{(cal/s)}$$

The overall freezing time can be estimated by dividing the heat of fusion to be removed by this heat removal rate,

$$t_F = \frac{C_F \, \pi d^3 \, (1 \text{ g/cm}^3) \, ( \, 1 - \Delta T \, C_P \, / \, C_F \, )}{6 \, R_H}$$

where $C_F \equiv$ heat of fusion (cal/g)
$C_P \equiv$ specific heat of water (1 cal/g/°C)
$\Delta T \equiv$ difference in ambient temperature and water freezing point (0°C)

The right hand term in the numerator takes into account the heat capacity of water gained in warming the droplet to 32°F (0°C) after ice nucleation. Combining these equations, one obtains

$$t_F = \frac{C_F \, d^2 \, ( \, 1 - \Delta T \, C_P \, / \, C_F \, )}{C_V \, \Delta n \, D_g \, 4 \cdot 10^{-22}}$$

This expression indicates that freezing time is proportional to the square of droplet diameter. The time also decreases with temperature as both $\Delta T$ and $\Delta n$ increase. Table 1 lists freezing times calculated for 20 μm diameter droplets at 28, 20, 0 and -30°F temperatures (with $D_g$ = 0.4 cm$^2$/s for water in air at 400 torr).

One should note that these estimates assume there is one nucleation site per droplet; large droplets may have multiple sites which could reduce estimated freezing times somewhat.

The $t_F$ values in Table 1 represent the times required to freeze the entire liquid volume of a supercooled droplet. In the context of anti-icing, these times and their corresponding distances at flight typical speeds represent upper limits for ice nucleation under flight conditions. The key question is: How much of a liquid droplet needs to freeze for the particle to bounce rather than accrete.

Table 1. Estimated Freezing Times and Flight Distances for 20 μm Diameter Droplet

| Temperature °F | Temperature °C | Water Vapor Pressure (torr) | Water Vapor Δn (mol/cm$^3$) | $t_F$ (sec) | Flight Distance 50 mph (meter) | Flight Distance 400 mph (meter) |
|---|---|---|---|---|---|---|
| 32 | 0 | 4.6 | 0 | | | |
| 28 | -2 | 4.0 | $2 \times 10^{16}$ | 0.16 | 3.5 | 28 |
| 20 | -7 | 2.7 | $6 \times 10^{16}$ | 0.06 | 1.2 | 10 |
| 0 | -18 | 1.2 | $10 \times 10^{16}$ | 0.03 | 0.6 | 5 |
| -30 | -34 | 0.2 | $13 \times 10^{16}$ | 0.015 | 0.3 | 2.5 |

## 1.6 Research Plan

The work plan of this project was based on the cooperative agreement of FAA and NASA personnel that made available the NASA LeRC IRT for ice accretion tests of ultrasonically induced ice nucleation. Based on discussions with NASA LeRC staff, it was decided to couple acoustic transducers with a flow duct mounted in the center of the IRT. The following general tasks were defined:

(1) Design and construct an assembly containing a total of nine acoustic transducers (and associated drive electronics) to cover the frequency range 10 to 650 KHz at power levels up to 120-130 dB.

(2) Design and construct a flow duct (8 x 2 x 1 feet) to be mounted in the center of IRT. Mount the transducer assembly a variable distance upstream of an airfoil. Distances (2 to 8 feet) were chosen to match expected freezing times as listed in Table 1.

(3) Monitor ice accretion on the airfoil as a function of transducer frequency and position. In order to maximize both ice nucleation and liquid freezing processes, start with coldest (-30°F) temperature, smallest (14 μm) droplet size and slowest (50 mph) air flow speed. Depending on results, vary experimental conditions to determine envelope of icing conditions.

Figure 2 shows a schematic of the apparatus as assembled and coupled with the NASA IRT facility.

The following three sections describe the apparatus, results and conclusions, respectively, of the testing measurements made in the NASA LeRC IRT during 17-19 December 1991.

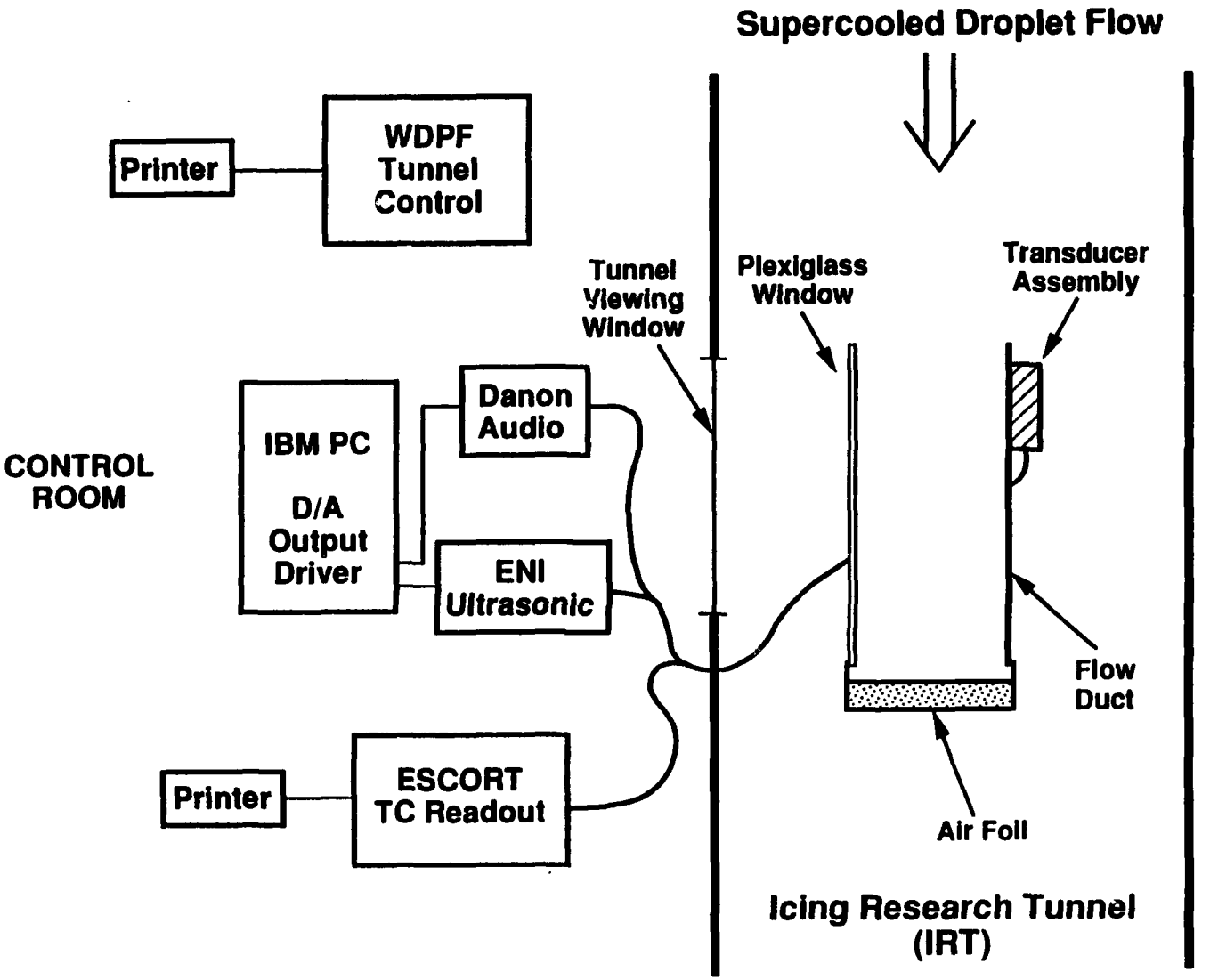


Figure 2. SCHEMATIC TRANSDUCER/FLOW DUCT APPARATUS IN THE IRT

## 2. APPARATUS

The experimental apparatus for these measurements is composed of a flow duct, an ultrasonic transducer array, power supplies and controlling electronics for the transducers, and computer control of the transducers and data logging. This apparatus was designed to be integrated with the NASA Icing Research Tunnel (IRT) facilities and significant design and fabrication support was provided by the IRT staff. The flow duct and transducer mounting plate were designed by ARI with significant input from IRT staff and both were built at NASA LeRC. The transducers and their control electronics were assembled and integrated with the NASA fabricated components and the entire assembly was mounted and tested in the IRT in the first day of the experimental program.

Beyond supplying the tunnel, test section, and flow with calibrated super-cooled droplet properties, NASA provided software for captioning the experimental results. Output from the operator console central tunnel control system (`WDPF')[10] was provided to log the tunnel conditions and the droplet spray system operating parameters. The transducer temperatures were monitored with thermocouples that were connected to the NASA LeRC data acquisition system (`ESCORT').[10] Print-outs of these temperatures provided a log of reference temperatures for each experimental condition.

### 2.1 Flow Duct

The flow duct is a 1 ft by 2 ft rectangular duct with three aluminum plate walls that is 8 ft in length, open at both ends (see Figs. 3,4). The fourth side of the duct is a 2 ft wall made of transparent lucite so that ice accretion on the walls and transducers can be monitored visually while the experiments are being performed. The purpose of this duct is to sample a clean flow with uniform velocity and water droplet properties near the center of the IRT test section and direct it toward the test airfoil located just beyond the open downstream end of the flow duct. The duct walls prevent any large scale residual swirl or cross flow from displacing and/or mixing the fluid that enters the duct before it impinges on the test airfoil. Thus, after the moisture-laden flowing air is exposed to the ultrasonic perturbations from the transducers , it will convect with minimal disturbances and mixing until it reaches the test airfoil.

The duct mounts on legs that bring the duct inlet into the uniform central region of the flow in the IRT test section (see Fig. 15 in reference 10). The power leads, thermocouple wires, and purge gas line are routed from the downstream end of the transducer cover, down one support leg, and through an opening in the tunnel floor, from which they travel into the IRT control room. There, the thermocouple wires connect to the `ESCORT' data acquisition system, the single-frequency transducer power cables connect to the ENI high-frequency power supply, and the broad-band transducers (tweeters)

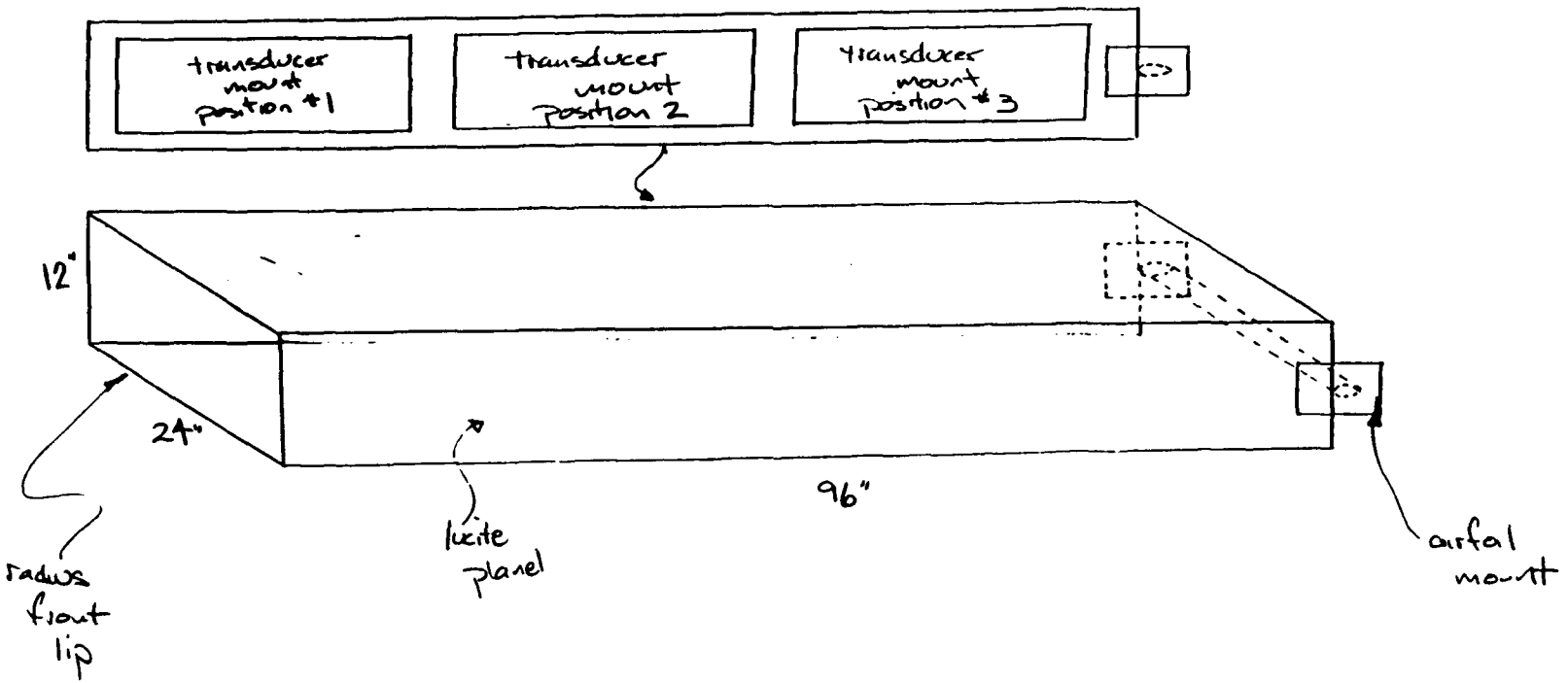


Figure 3. ROUGH DESIGN SKETCH OF THE FLOW DUCT
The overall dimensions, the possible locations of the transducer mounting plate, and the airfoil attachment method are shown schematically.

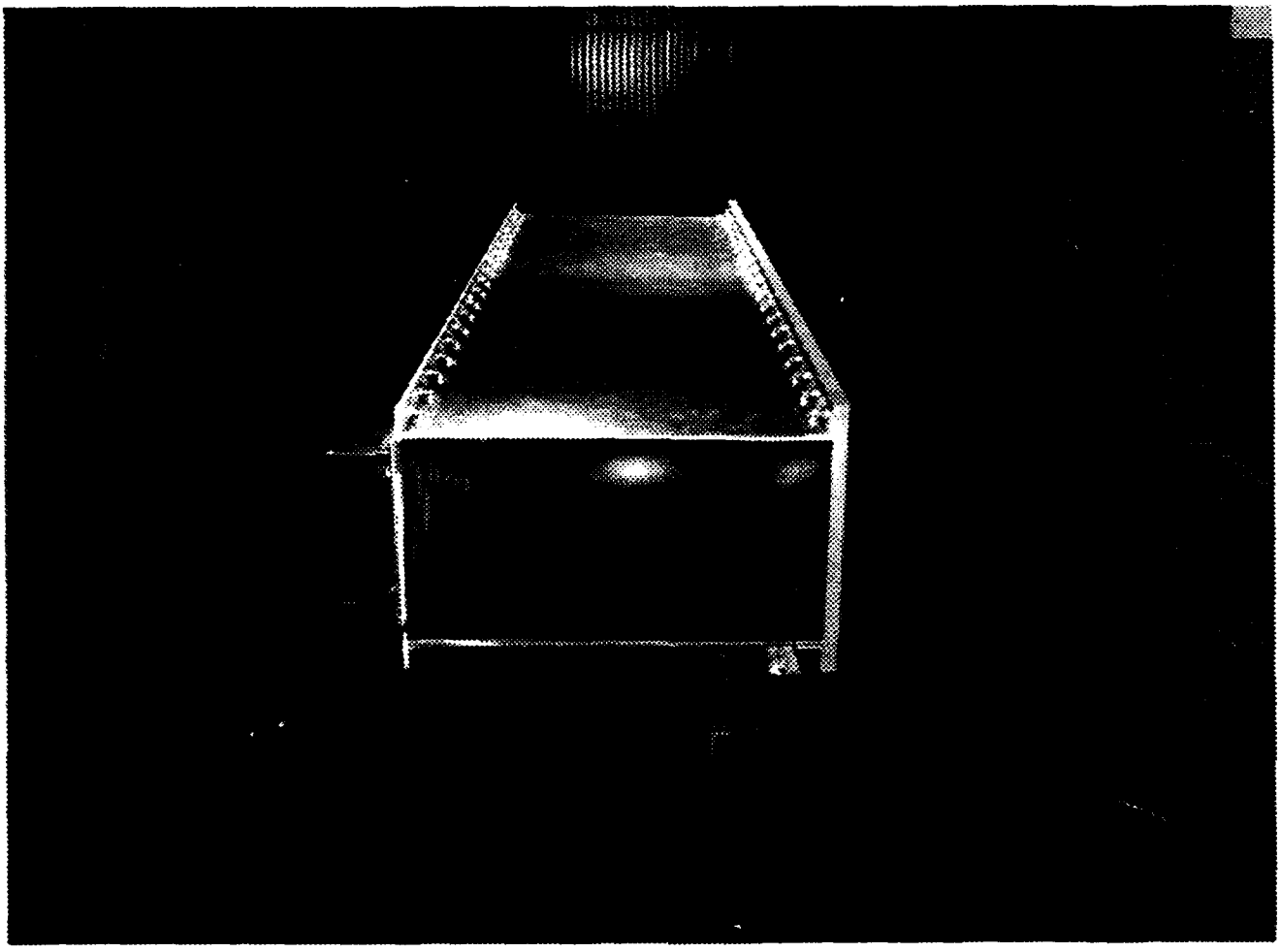

Figure 4. FLOW DUCT MOUNTED IN IRT TEST SECTION
The 8 foot long flow duct is mounted near the center of the 6' by 9' cross section of the 20' deep test section. The transparent face of the duct is on the right in this photograph, taken looking downstream, and is directed toward the control room viewing windows which are visible at the right edge of the photo.

are connected to an extended-range audio amplifier which powers them.

## 2.2 Airfoil

The test airfoil is mounted on plates (see Fig. 5) that attach to the 30 cm duct walls and position the airfoil in the center of duct cross section along its long (61 cm) transverse axis. The leading edge of the airfoil is displaced from the trailing edge of the duct so that ice accretion can be observed visually during a test without interference from duct walls. Three different airfoils were assembled, with chords ranging from 3.0 cm to 8.6 cm. The 8.6 cm airfoil was used in the measurements reported. Reference lines along this airfoil's span allow the span-wise variation in ice accretion to be quantified. The airfoil assemblies use streamlined steel tubing welded to steel endplates to form a rigid structure that aligns the symmetric airfoil in the flow direction.

## 2.3 Transducer Assembly

The transducers are mounted in an assembly that mounts flush to the aluminum 30 cm wall of the flow duct (opposite the lucite wall). The transducer assembly can be mounted in any of the three locations along that wall, allowing the distance (and thus the time, for a given flow velocity) between the transducer excitation and the airfoil to be selected. Shorter distances and times can be used to explore the temporal dependence of droplet freezing, with the longest distance chosen as the initial test condition as used in these experiments.

**The transducer assembly (Figs. 6,7) accepts an array of transducers of four different frequency characteristics and multiple transducers of each type were used in these experiments. The higher ultrasonic frequencies were generated by pairs of three different, single-frequency transducers operating at, nominally, 80 kHz, 350 kHz, and 650 kHz. Each of these pairs were arranged so as to illuminate a streamtube that flows to the test airfoil. One transducer is displaced a little above and the other is displaced equally below the dividing streamline so that the entire streamtube impinging on the airfoil is illuminated. This staggered arrangement of the transducers ensures that even with a reasonable amount of turbulent mixing in the duct (which has been relegated to smaller turbulent length scales by the confining effects of the duct), the fluid impinging on the airfoil has been illuminated with the excitation energy.**

**The three pairs of staggered single-frequency transducers are followed by a set of three high-frequency audio loudspeakers (Dynaudio D-21F tweeters) that are capable of generating ultrasonic excitation up to 40 kHz. Unlike the single-frequency transducers, these tweeters are broad-band and very uniform in**

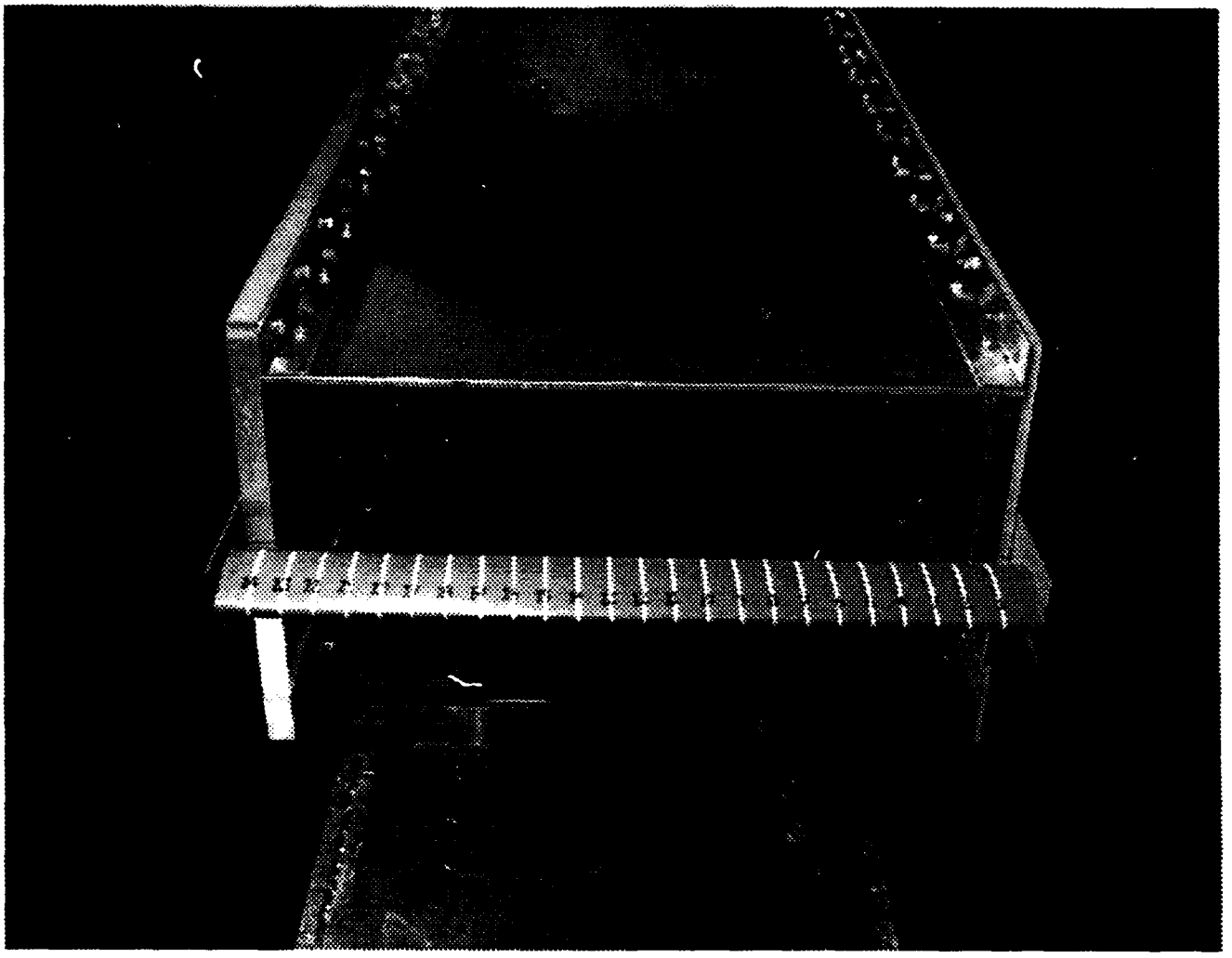

Figure 5. AIRFOIL MOUNTED TO FLOW DUCT
The 3.375 inch chord airfoil, composed of streamlined tubing welded to two mounting end plates, is shown attached to the downstream (exit) end of the flow duct. The transducer mounting plate is attached to the aluminum wall on the righthand side of this photograph, taken upstream of the test section. The transducers are at the upstream end of the flow duct and are thus out of view in this photo.

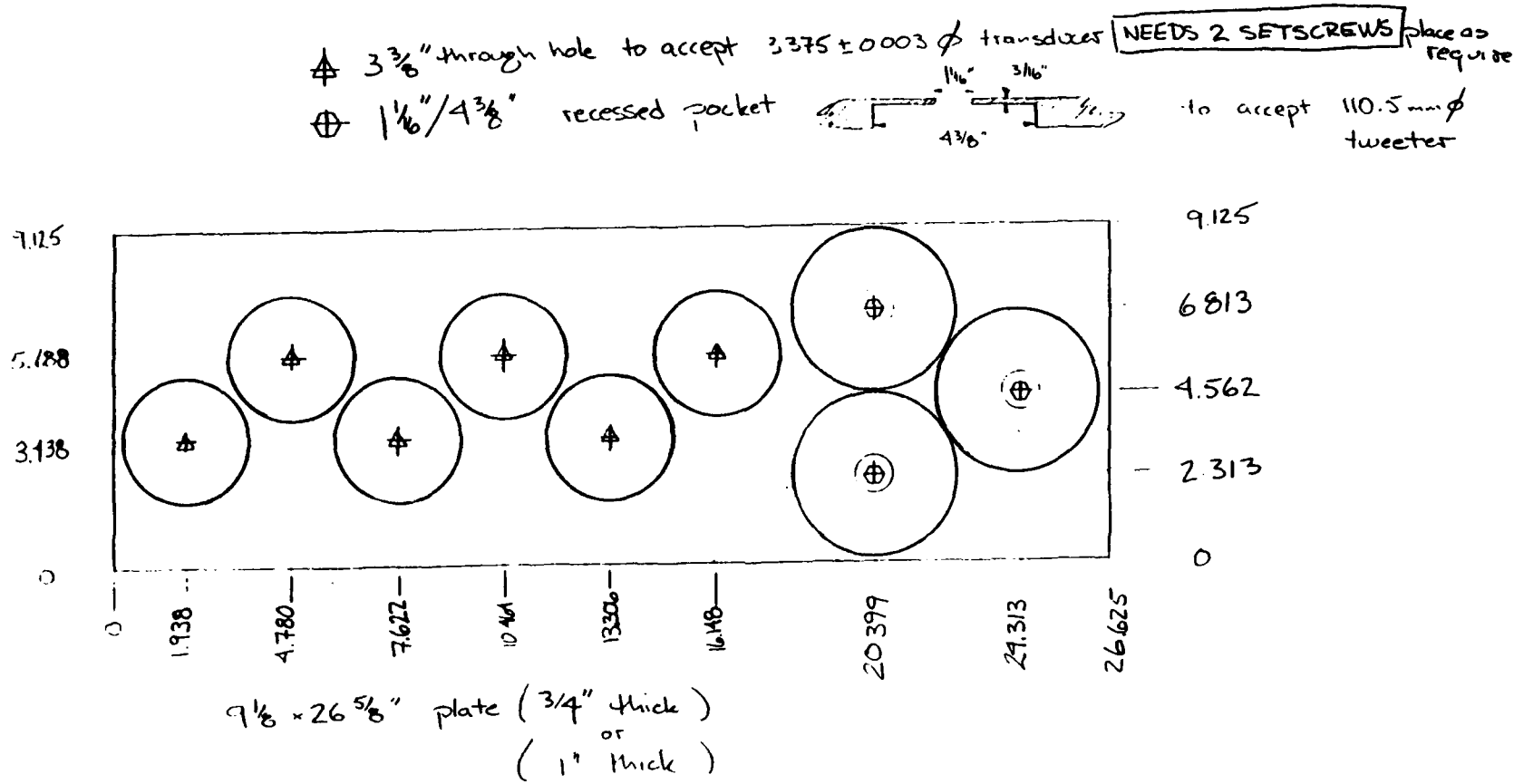


Figure 6. ROUGH DESIGN SKETCH OF THE TRANSDUCER MOUNTING PLATE
The overall dimensions, transducer locations, and the mounting methods are shown schematically.

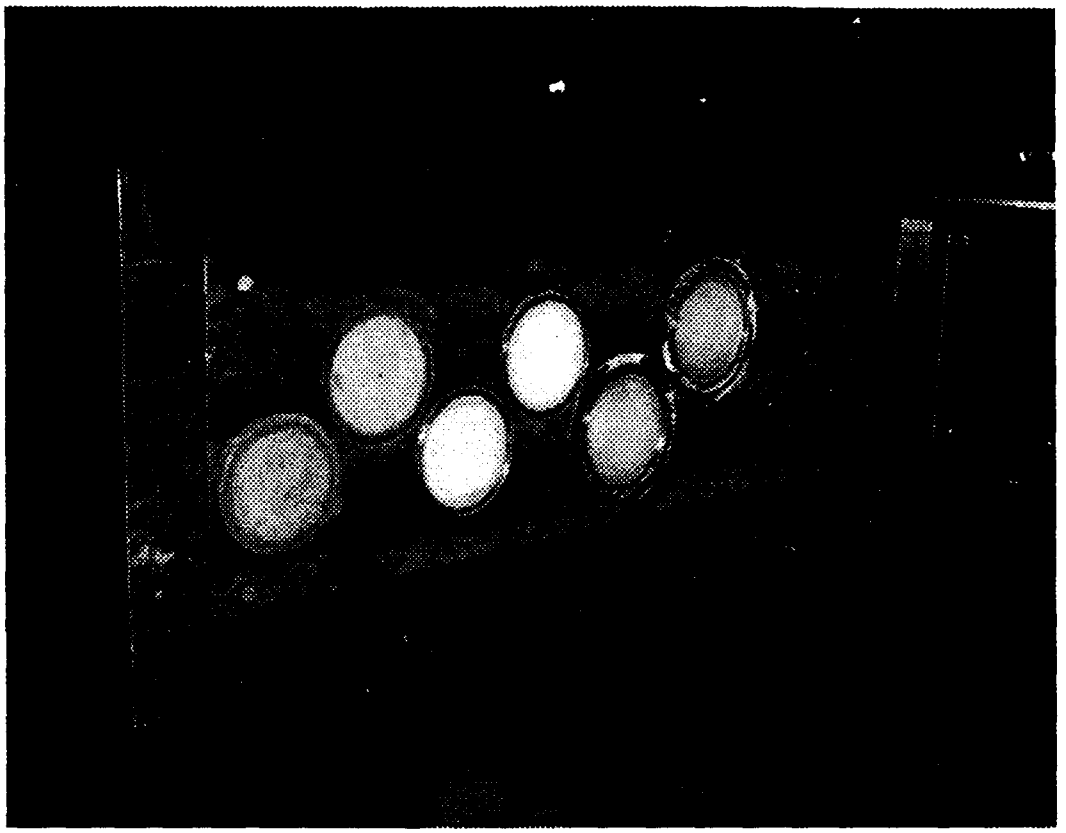

Figure 7. THE TRANSDUCER ASSEMBLY IN PLACE IN THE FLOW DUCT
The six single-frequency transducers, two each of 650 kHz, 350 kHz, and 80 kHz from left to right in the photograph, are positioned in overlapping pairs to ensure good excitation coverage of the central flow down the duct. The broadband tweeters (20 kHz - 40 kHz) are barely visible to the right of the 80 kHz transducers. The dry purge gas slot is visible just to the left of the leftmost 650 kHz transducer.

their response. Their major limitation is that the total power they can deliver is the sum or integral across the input frequency bandwidth, meaning that the power available at any given frequency is diminished by the power simultaneously delivered at all other frequencies . The three tweeters are arranged with one on the duct centerline and one on each side, again to minimize the effects of unexcited fluid mixing into the impinging streamtube from the sides due to turbulent fluctuations.

The transducers and their impedance-matching components (see below) are set in the mounting plate with the emitting faces of the transducers aligned to the flow-exposed surface of the plate. The components and connections on the other side of the plate are protected from the droplet-laden IRT flow by a sheet metal cover that is sealed to the back of the mounting plate. The transducer power connections are made through bulkhead BNC fittings in the downstream cover wall, while the thermocouple connections to the transducer temperature sensors run through an opening in this wall, which is sealed during mounting. A Polyflo bulkhead feedthrough is used to provide dry purge gas for the transducers.

The dry-gas purge is used for two purposes. The first is to prevent moisture from accumulating on or around the electrical connections to the transducers. To do this, the entire internal volume contained inside the cover is purged with the dry-gas flow. Thus, even though the cover is sealed, any leaks and resultant condensation of existing water vapor will be swept out of the cover. The purge flow leaves the volume behind the mounting plate through a slot in the front of the mounting plate itself, venting into the flow duct at the upstream end of the transducer array (see Fig. 7). This provides a second use of the dry purge gas.

By injecting dry purge gas into the boundary layer along the transducer mounting plate, the transducer faces are afforded some protection from ice accretion due to the droplet-laden IRT flow. After performing the experiments, it became apparent that this protection was minimal, which may have as much to do with the dynamics of ice accretion as with turbulent mixing through the boundary layer. In any case, for dry-gas injection levels that did not significantly perturb the duct flow, ice accretion was not prevented on the transducer faces and the wall downstream of the injection slot. The accretion that was observed was not large and coverage was spotty, growing as whiskers on this surface parallel to the flow, and was cleaned after each run.

## 2.4 Control Electronics

The ENI high-frequency power supply used to drive the single-frequency transducers has a 50 Ohm output impedance. The transducers, on the other hand, have a complex impedance that is a rapidly varying function of frequency near the respective resonant design frequencies (Figs. 8 a,b,c). To optimally excite the flow

with the maximum power, the transducers were impedance matched to the output amplifier of the ENI at their particular frequency by incorporating a (remotely located) high frequency transformer and an appropriately chosen inductor to offset the transducer's capacitance at that frequency. A high value bleed resistor was also wired in parallel to the transducer since these devices also demonstrate pyroelectric behavior and develop significant capacitive charge when cycled in temperature, particularly for the extreme temperature variations in the IRT. This small electronics package is mounted on the back of each single-frequency transducer along with a BNC connector, that provided the means of connecting to the power distribution cables.

Most of the transducers were delivered to Aerodyne with a K-type thermocouple imbedded in the potted assembly in contact with the piezoelectric ceramic. This was used to monitor the level of power that could be delivered to each transducer. The transducer manufacturer specifies that the transducers should be capable of withstanding ceramic temperatures to 100°C. The low temperatures in the IRT allowed much higher power levels to be delivered to the transducers than were possible in tests at room temperature.

The tweeters had a broad-band frequency response from 1 to 40 kHz. They were also fitted with thermocouples, placing the junctions as close to the voice coil as possible. While the temperature of the voice coil itself was not measured, and heating is the ultimate failure mode of these devices, the measured temperature increased very quickly as the damage threshold was approached. Thus operation within several dB of the damage power level was possible, allowing a near maximal excitation power to be used.

A microcomputer-based system provided the frequency selection and signal generation. Software was developed for these experiments that selected a set of frequencies for all the transducers that would match their individual resonance characteristics. These frequencies were then generated simultaneously on two plug-in D/A frequency-generator boards (Quatech, Inc.); one generated the set of frequencies for the higher single-frequency transducers and the other generated a set of frequencies to be delivered to each of the broad-band tweeters.

## 2.5 Transducer Power Supplies

The driving signals for all the single-frequency transducers were amplified by a ENI high-frequency power amplifier. This device's power output (>100 W 30 kHz-4 MHz) exceeded the sum of the power requirements of the transducers, but only if their impedances were matched to the 50 Ohm amplifier output. Thus the multi-frequency output of the ENI amplifier was fed to a high-frequency transformer with output for the different transducer types taken from appropriate transformer taps (different for each type). The

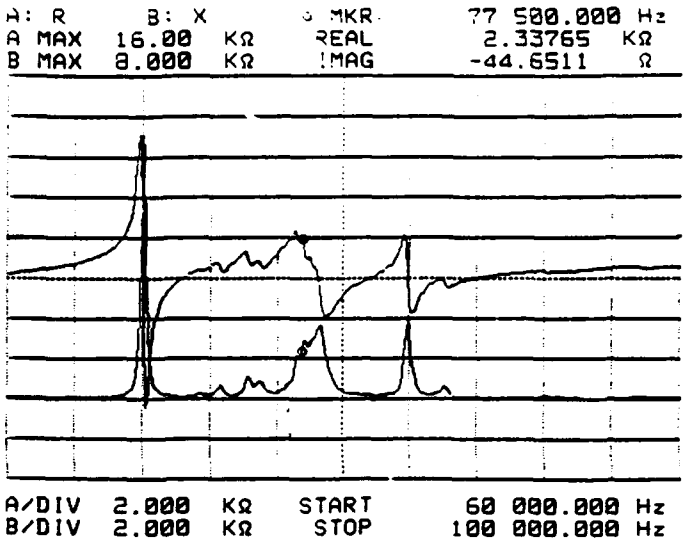


(a)

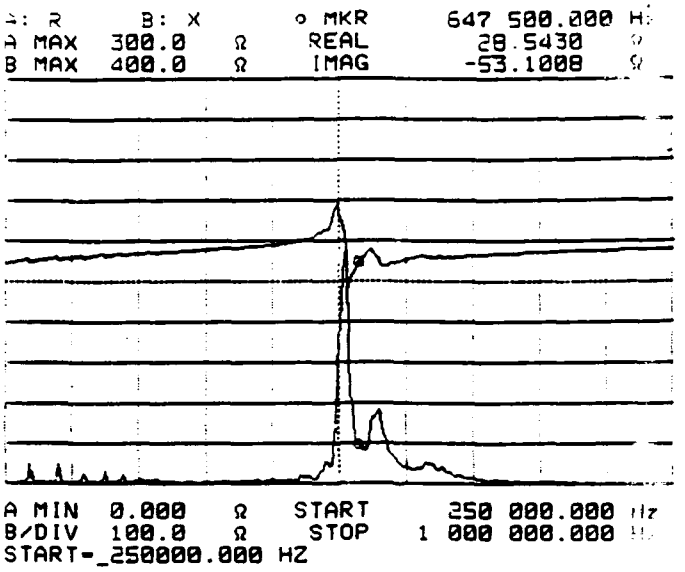


(b)

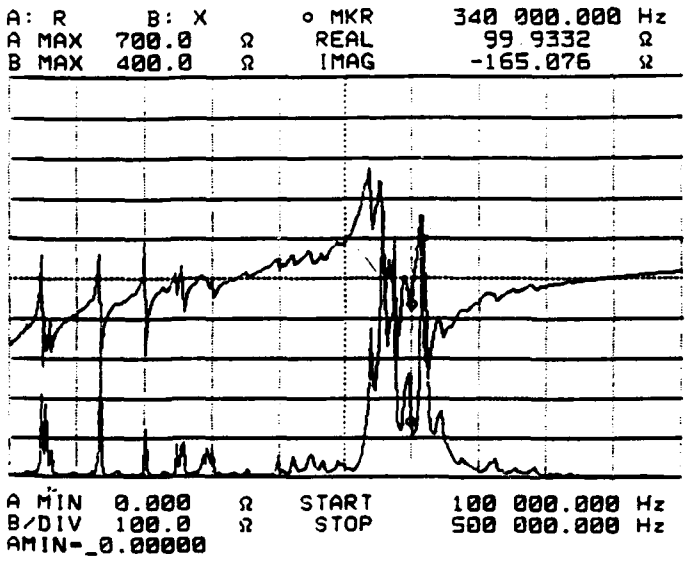


(c)

Figure 8. FREQUENCY RESPONSE CURVES FOR THE PIEZOELECTRIC TRANSDUCERS

The complex impedance (imaginary [capacitive] component is upper curve, real [resistive] component is lower curve) for the three transducers is plotted versus frequency about the nominal design frequency. The individual plots represent a) 80 kHz, b) 350 kHz, and C) 650 kHz.

amplified signal was delivered to the inductor/resistor/transducer assembly via coaxial cables and connectors.

The tweeter band (20-40 kHz) extends just beyond the audible range, so a commercially available audio amplifier was used to amplify those signals. A Denon POA-2800 stereo amplifier was selected since it has good response beyond the high-frequency cut-off of the tweeter transducers. Even though both the tweeters and amplifier are considered to be expensive audio equipment due, in part, to their high frequency response, their costs were significantly lower than other low frequency options.

## 2.6 Experimental Approach

Ice accretion experiments were performed by exposing the airfoil at the end of the flow duct to supercooled droplet flow in the wind tunnel for ten minute periods. Ice accretion thickness would then be measured, the airfoil cleaned, and another run started. The output of the acoustic transducers was kept constant during each run. Transducer parameters were systematically varied from run to run. More details in the procedures followed for each experimental run are described below.

Starting with a clean airfoil, the IRT staff would increase tunnel flow to the desired speed and stabilize the temperature throughout the tunnel. This stabilization would take 5-10 minutes, with temperature profiles measured between the water spray bars and the test section of the tunnel being constant within 1-2°F. The water spray would then be turned on for precisely ten minutes. During that time the airfoil was visually monitored through the viewing window in the control room as well as videotaped through a ceiling window.

Operation of the transducers was monitored electronically on an oscilloscope and via a panel meter on the ENI amplifier. Driving voltage was increased (via computer control) until waveform distortion was observed as the amplifier was driven to its limit. Actual transducer driving power was checked via the temperature rise of thermocouples mounted in the ultrasonic piezoelectric transducers and on the surface of the tweeters. Temperatures of the former were usually in the range 30-60°F. This was much lower than the rated maximum of 212°F, indicating that, in the cooling flow of the IRT, power levels were limited by the amplifier and imperfect impedance matching.

After the ten minute exposure time, wind tunnel speed was idled down to 10 mph and the access door opened to allow ARI and NASA personnel to enter the tunnel. Polaroid and 35mm color still pictures were taken both of the airfoil and the transducer assembly. Figure 9 shows two such pictures for ice accretion runs at 0°F and -36°F. Ice accretion on the front edge of the airfoil (pointing toward the left into the flow duct) is clearly visible.

Those pictures show two extremes in ice accretion profiles. By comparing the two, one can see that the upper picture (a) corresponds to a thick ice layer (up to 0.6" deep). At the bottom of (a), one can clearly see the reduced ice accretion near the flow duct wall due to expected boundary layer effects. Accretion in the center section of the airfoil is somewhat uniform (see Figure 13). In the lower picture (b) there is obviously much less ice accretion (cf. Figure 14), due to homogeneous freezing of droplets in the wind tunnel (see Sections 3 and 4).

Ice accretion thicknesses were determined manually by using a pair of calipers to measure the distance between front of the ice to the back of the airfoil. Ice thickness is then given by the difference between that distance and the 3.375" chord of the airfoil. For most experiments, the ice thickness was measured at 13 points along the airfoil, as marked by the numbered strips visible in Figures 5 and 9.

After measuring ice thickness, the airfoil was cleared of ice. The surfaces of the transducers at the front of the flow duct were also carefully brushed to keep them free of ice buildup. During a series of runs, ice continued to build on the interior surfaces of the flow duct. This can be seen in Fig. 10, which shows a photograph from a front view of the flow duct after an ice accretion run. This build-up had little apparent effect on ice accretion profiles on the airfoil. This was consistent with boundary layer calculations that predicted a stable centerline flow in the duct.

After clearing the ice from the test fixture and closing the access door, tunnel speed was increased and a new icing run started on the clean airfoil. During tunnel stabilization, the results of the ice accretion measurements were plotted on a laptop microcomputer to provide real time presentation of the data. The total time required for an ice accretion run was on the order of 30-45 minutes.

(a)

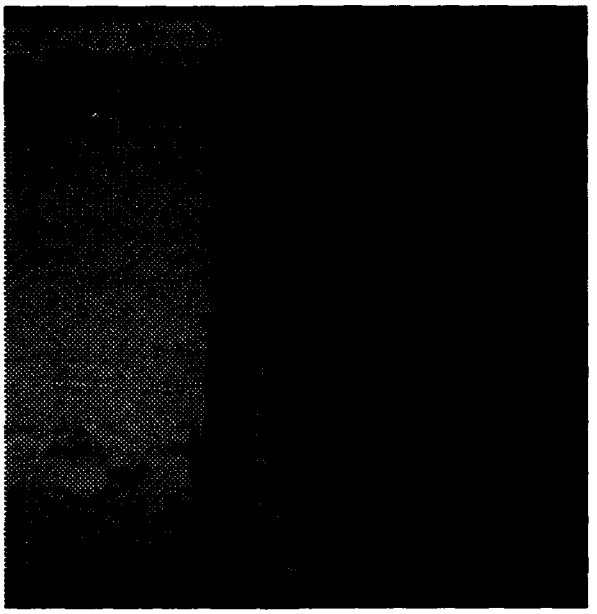

(b)

Figure 9. ICE ACCRETION ON 3.375 INCH AIRFOIL
The ice accretion for Runs (a) 2-4 (0°F) and (b) 4-1 (-36°F) was photographed at the end of the 10 min run time. The minimal accretion in (b) is attributed to freezing of the droplet cloud at the low tunnel temperature. In (a), the depletion of the ice at the ends of the airfoil is due to liquid water content (LWC) losses through the duct boundary layer and deposition on the walls.

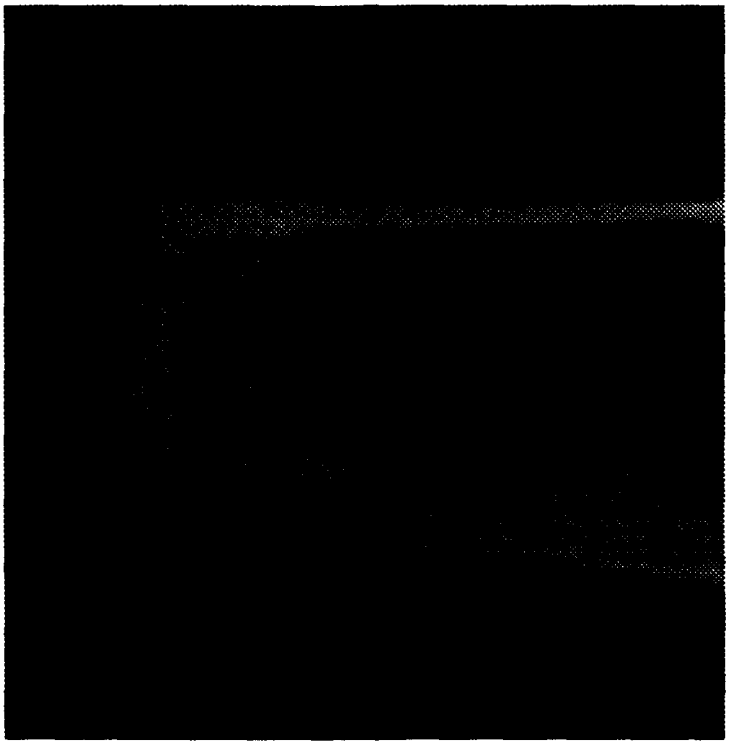

Figure 10. ICE BUILD-UP IN INTERIOR OF FLOW DUCT
Photograph from front of flowduct taken after Run 3-5. Ice accumulation on interior surfaces was clear, though continuing build-up had little apparent effect on accretion on airfoil. Transducer assembly was relatively clear, since it was brushed clean between runs. Ice accretion on the faces of the active (340 KHz) transducers was minimal (see p. 32,38).

# 3. ICE ACCRETION RESULTS

## 3.1 Research Chronology

On 17 October 1991 a kickoff meeting was held at the NASA Lewis IRT facility. FAA, NASA and ARI personnel participated. That meeting focused on the design of the flow duct / transducer assembly. Based on decisions at that meeting, ultrasonic and audio transducers were specified and ordered. Over the next two months, on-going telephone discussions between ARI and NASA personnel led to the final apparatus configuration schematically shown in Figure 2 and discussed in Section 2. NASA personnel were responsible for construction of the flow duct, while ARI designed and built the transducer assembly and its associated electronics, including hardware and computer software.

Planning also resulted in formulation of the test plan flowchart shown in Figure 11. This involves variation of IRT parameters (flow speed, temperature, liquid water content (LWC), droplet size) and transducer parameters (frequency, power level), depending on ice accretion observations. As mentioned at the end of Section 1, initial conditions were chosen to optimize ice nucleation and liquid freezing rates: the coldest temperatures, slowest tunnel speed and smallest droplets.

The ultrasonic transducers arrived at ARI on 9 December 1991. That week was spent integrating the transducers with the computer controlled audible and ultrasonic amplifier electronics. System testing focused on impedance matching of the ultrasonic transducers. On 13 December 1991 the transducers and associated electronics were shipped air freight to NASA LeRC.

ARI and FAA personnel arrived at NASA LeRC on 16 December 1991. That day was largely spent integrating the transducers with the mounting block supplied by NASA. Simultaneously, NASA personnel mounted the flow duct in the IRT and ARI personnel installed the computer and acoustic amplifier drivers in the IRT control room. That night a preliminary run in the IRT served to certify the aerodynamic stability of the flow duct and demonstrate rates of ice accretion on the air foil at the end of the flow duct.

On the nights of 17-18 December 1991, a total of 23 ice accretion measurement runs were made in the IRT, 13 with various combinations of transducers ON and 10 with all transducers OFF. The latter 'null' runs were necessary in order to establish a baseline of unperturbed ice accretion rates. Review of the data resulting from the tests of 17-18 December exhibited negative results. Discussions with NASA personnel on the morning of 19 December resulted in the decision to discontinue testing.

Overall, the test apparatus worked well and performed very close to plan. There were on-going problems with impedance matching

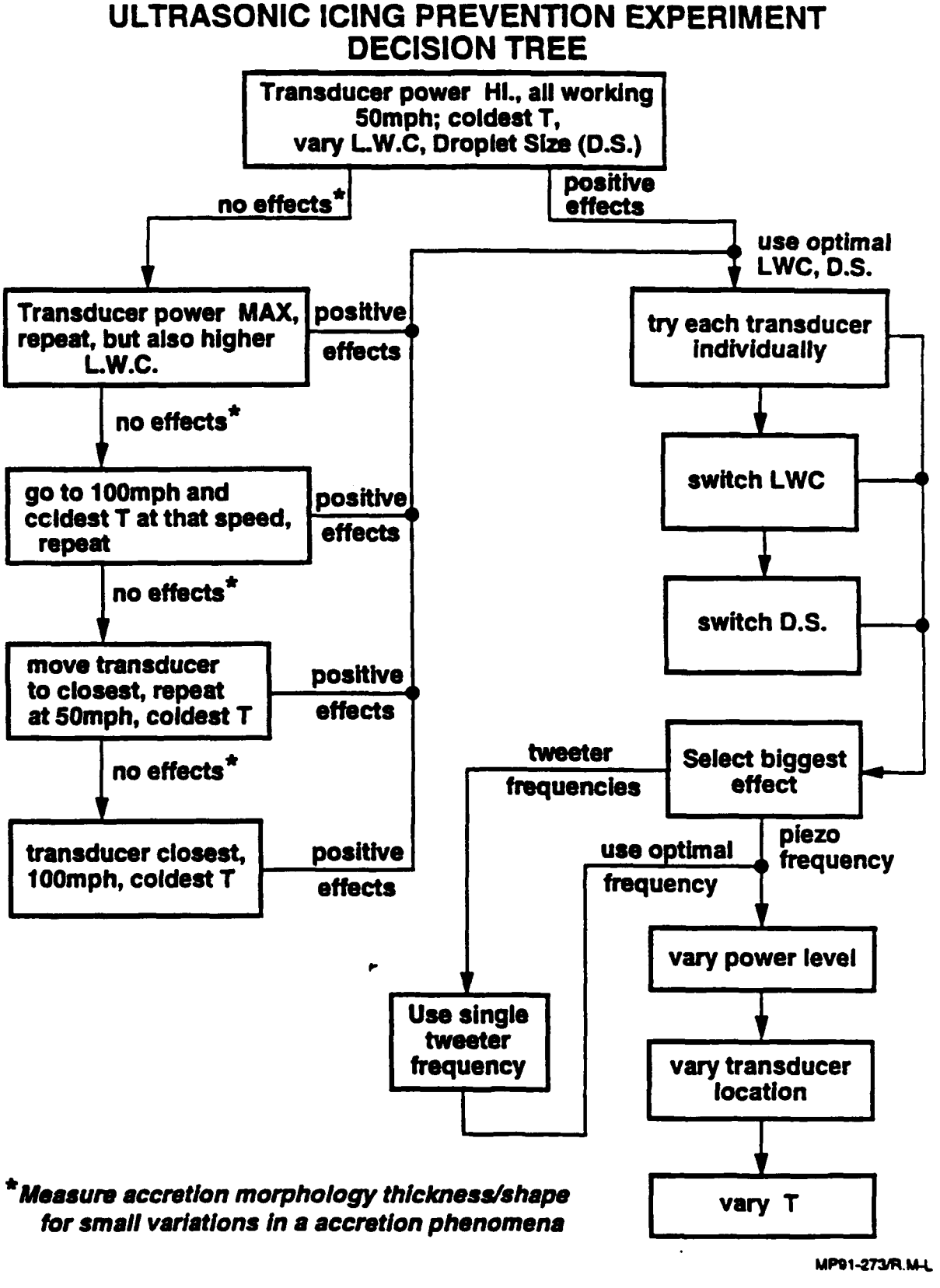


Figure 11. EXPERIMENTAL TEST PLAN FLOW CHART

of the ultrasonic transducers which limited acoustic output power levels. It also became apparent that cooling from the IRT air flow could allow driving of the transducers at power levels beyond the capabilities of the single ENI ultrasonic amplifier. It was clear that improvements in design could lead to enhancements in acoustic output power levels.

In the remainder of Section 3, the actual measurements made and their analysis/interpretation are described in detail. Section 4 discusses in more detail the conclusions and implications of the failure to observe any acoustically induced reduction in ice accretion.

## 3.2 Ice Accretion Measurements

Table 2 summarizes the conditions of the 23 runs performed in the IRT. Figures 12-14 plot ice accretion thickness (measured as described in Section 2.6) as a function of position along the airfoil with zero corresponding to the transducer assembly side of the flow duct. Figure 15 plots the average ice accretion thickness in the center 16 inches (4 to 20 in Figures 12-14). The x-axis has no physical significance. The points are plotted simply in the order in which the runs were performed. In all figures, transducer ON/OFF runs are identified as labeled.

**As labeled in Figure 14, the defining parameter for the four sets of runs was the wind tunnel temperature, which was varied between 0°F and -36°F. In accordance with the left ('no effects') side of the test matrix (Figure 11), liquid water content (LWC) and flow speed were also varied, as listed in Table 2 and labeled in Figures 12-14. The chronology of the different runs is described below.**

Set 1 was acquired on the night of 17 December at a tunnel temprature of -20°F. The first four runs were at 50 mph, the first and last (1-1 and 1-4) with the transducers OFF. The next five runs were at 100 mph flow speed, with the first (1-5) again being run with the transducers OFF. Since there was no significant change in the ice accretion , it was decided to run at the slower 50 mph for all subsequent runs to maximize time available for droplet freezing (see Table 1).

Likewise, the results of Set 1 established the pattern of transducer power levels for subsequent runs. Run 1-2 distributed acoustic power among 20, 25, 30, 35, 40, 340 and 650 kHz frequencies. At that time it became apparent that impedance mismatches interfered with simultaneous operation of the ultrasonic transducers. In view of the lack of any acoustically induced effect, it was also decided to concentrate the power by driving the tweeters at one frequency. Thus, in all subsequent transducer ON

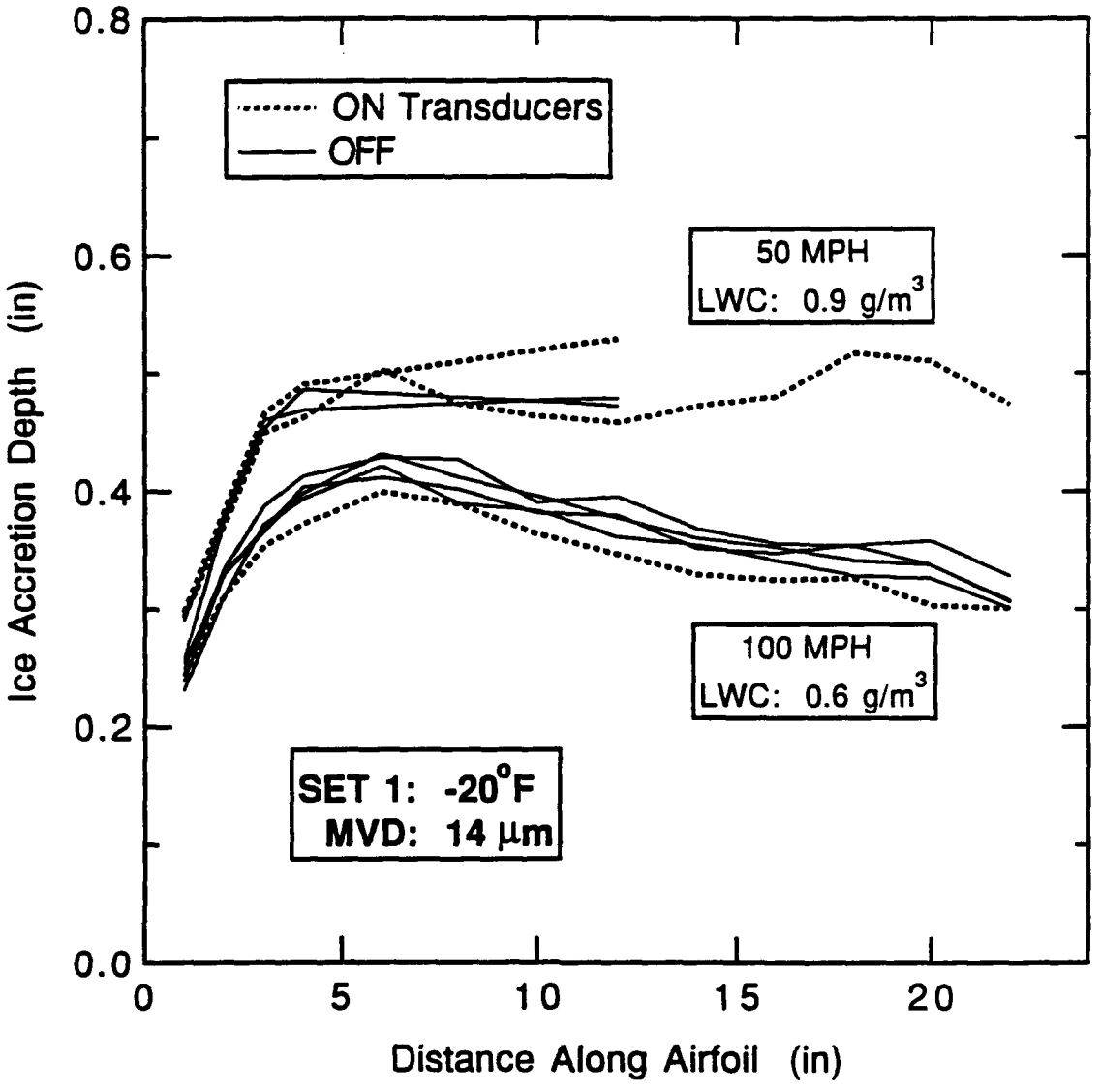


Figure 12. ICE ACCRETION PROFILES FOR DATA SET 1
The accreted ice thickness is plotted at 1 inch increments along the airfoil span, measured from the duct wall in which the transducers were mounted. Depletion at the edges is due to boundary layer effects. The first three profiles only extend to the midpoint, after which the possibility of profile asymmetry prompted taking measurements along the full airfoil span. The 100 mph data, at reduced LWC, corresponds well with the 50 mph data and the lower speed was used for subsequent runs to maximize the time available for droplet freezing.

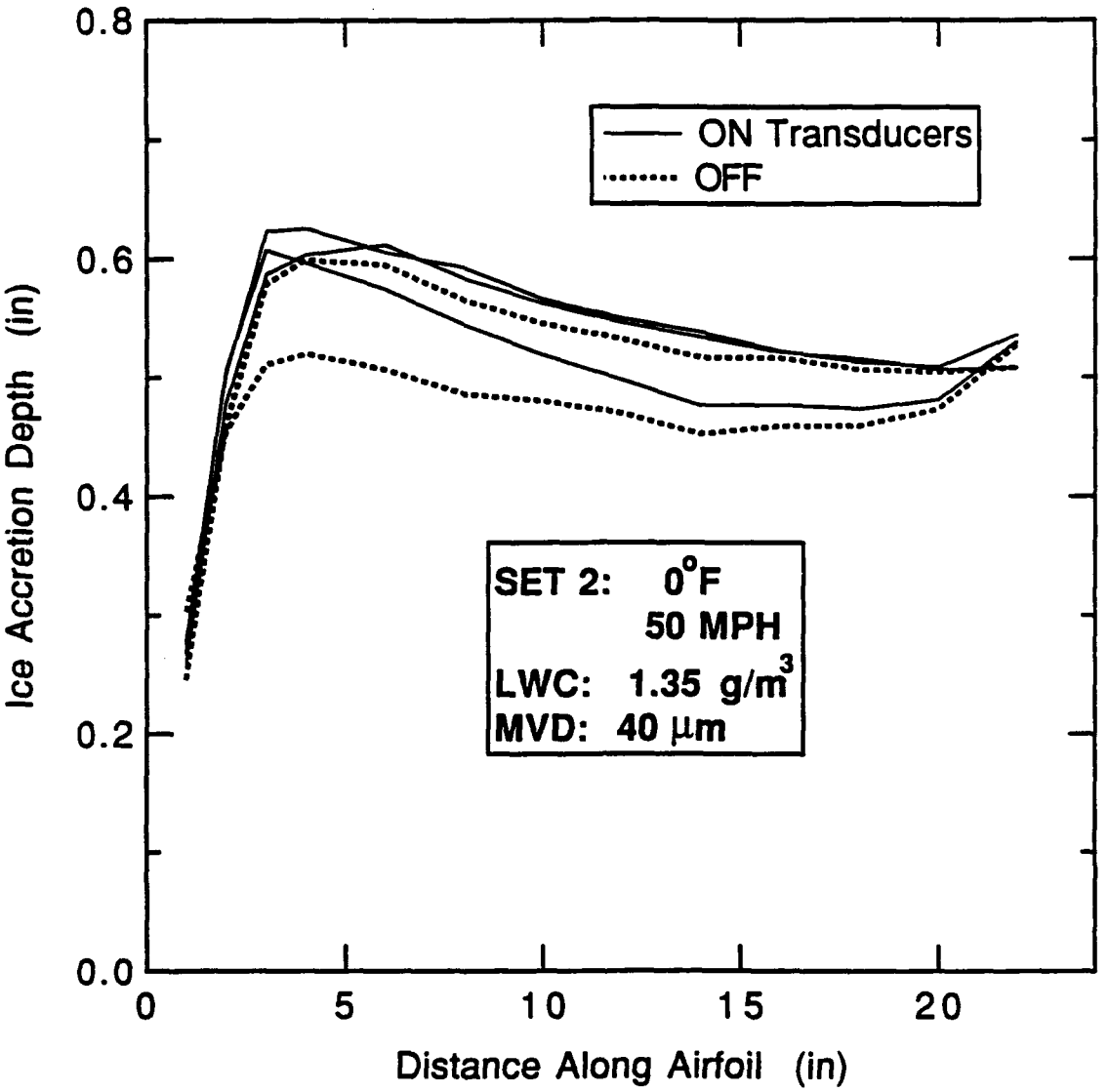


Figure 13. ICE ACCRETION PROFILES FOR DATA SET 2
The lowest profile, with the transducers OFF , was the first run for these conditions and apparently represents non-equilibrium conditions in the tunnel. Variations in the subsequent runs indicate the reproducibility of these measurements.

TABLE 2. SUMMARY OF IRT RUN PARAMETERS

| Date | Run | Start Time | T (°F) | Vel (mph) | LWC (g/m³) | MVD (μm) | Power (Watts) | | | | | | | Average Ice Thickness (inches) |
|---|---|---|---|---|---|---|---|---|---|---|---|---|---|---|
| | | | | | | | Tweeters | Transducers | | | | | | |
| | | | | | | | Frequency (kHz) | | | | | | | |
| | | | | | | | 10 | 20 | 40 | 80 | 340 | 650 | | |
| 12-17 | 1-1 | 16:35 | -22.2 | 50 | 0.9 | 14 | - | - | - | - | - | - | OFF | 0.510 |
| | 1-2 | 17:35 | -19.6 | | | | | 7.5[a] | 7.5[a] | - | 10 | 10 | | 0.479 |
| | 1-3 | 18:14 | -19.6 | | | | - | 15 | - | 30 | - | - | | 0.474 |
| | 1-4 | 18:55 | -19.8 | | | | - | - | - | - | - | - | OFF | 0.482 |
| | 1-5 | 19:32 | -19.9 | 100 | 0.6 | | - | - | - | - | - | - | OFF | 0.351 |
| | 1-6 | 20:16 | -20.1 | | | | - | 15 | - | 50 | - | - | | 0.366 |
| | 1-7 | 20:53 | -20 | | | | - | - | 15 | - | - | 32 | | 0.378 |
| | 1-8 | 21:30 | -20 | | | | - | - | 30 | - | - | 60 | | 0.385 |
| | 1-9 | 22:09 | -19.6 | | | | 80[b] | - | - | - | - | 32 | | 0.376 |
| 12-18 | 2-1 | 15:07 | 1.1 | 50 | 1.35 | 40 | - | - | - | - | - | - | OFF | 0.478 |
| | 2-2 | 15:45 | 0.4 | | | | - | - | 20 | - | 60 | - | | 0.515 |
| | 2-3 | 16:17 | 0 | | | | - | 30 | - | 45 | - | - | | 0.558 |
| | 2-4 | 16:14 | 0.1 | | | | 25 | - | - | - | - | 40 | | 0.553 |
| | 2-5 | 17:08 | 0.3 | | | | - | - | - | - | - | - | OFF | 0.542 |
| | 3-1 | 17:52 | -31.9[c] | 50 | 1.35 | 40 | - | - | - | - | - | - | OFF | 0.305 |
| | 3-2 | 18:32 | -29.8 | | | | 25 | - | - | - | - | 40 | | 0.596 |
| | 3-3 | 19:00 | -30.0 | | | | - | - | - | - | - | - | OFF | 0.664 |
| | 3-4 | 19:26 | -30.2 | | | | - | 27 | - | - | 60 | - | | 0.612 |
| | 3-5 | 20:13 | -30.6 | | | | - | - | 20 | 70 | - | - | | 0.621 |
| | 3-6 | 20:35 | -30.0 | | | | - | - | - | - | - | - | OFF | 0.656 |
| | 4-1 | 21:18 | -35.6 | 50 | 1.35 | 40 | - | - | - | - | - | - | OFF | 0.076 |
| | 4-2 | 21:50 | -35.9 | | | | 25 | - | - | - | - | 40 | | 0.093 |
| | 4-3 | 22:12 | -35.6 | | | | - | - | - | - | - | - | OFF | 0.129 |

[a]Tweeter power actually evenly distributed at 20, 25, 30, 35 and 40 kHz (3 watts each).
[b]Tweeters failed during Run 1-9 at this high power level.
[c]Run 3-1 ~2°F below -30°F target because of IRT temperature programming error.

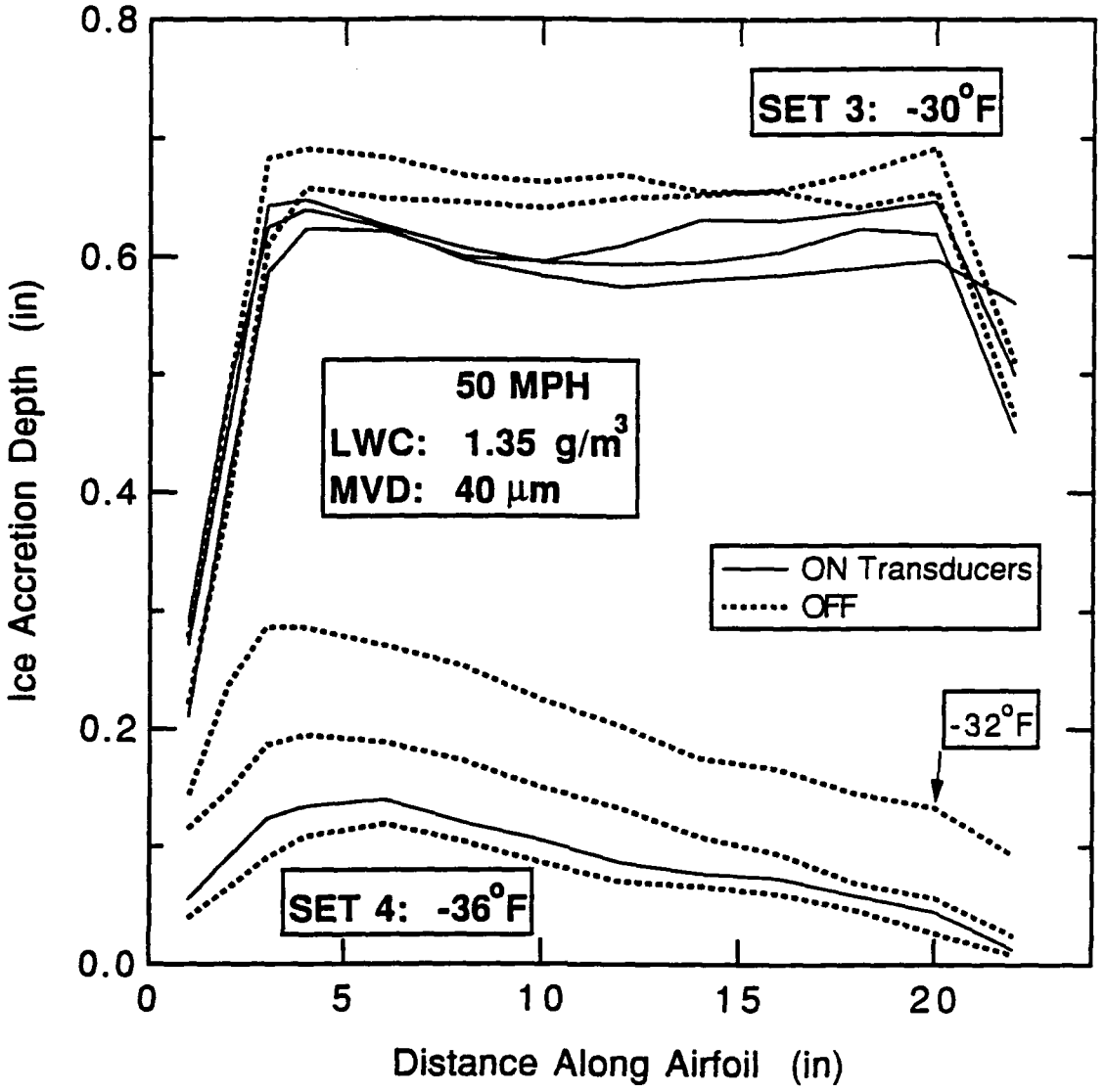


Figure 14. ICE ACCRETION PROFILES FOR EXPERIMENTAL DATA SETS 3 AND 4 These experiments were run at the coldest temperature achievable in the IRT . The controlling software was programmed to take the tunnel to -30°F but, in fact, overshot to -32°F for the first run of set 3. After warming to a true -30°F, the software was modified by IRT operators and -36°F was achieved for run 4. Such cold temperatures had not been previously maintained in the tunnel with its current system control unit.

runs the tweeters were driven at a single frequency (10, 20 or 40 kHz) while driving one pair of the single frequency ultrasonic transducers. During the last run (1-9) on 17 December the tweeter power was increased to 80 watts at 10 kHz. Sometime during the run the tweeters failed. This was consistent with maximum power levels specified by the manufacturer. Thus, the tweeters were replaced during the morning of 18 December. Also, it had become clear that one of 650 kHz transducers was emitting low power, probably due to severe impedance/resonance mismatch with the other. Thus, that transducer was replaced with the 650 kHz spare, which did indeed perform better.

The performance of the ultrasonic transducers could also be monitored by the amount of ice accretion on their front surfaces at the end of a run. The transducers that were ON were virtually clear of ice. In the case of the defective 650 kHz transducer, the improved performance of the replacement on the second night was easily observed from reduced ice accretion on its front surface. A temperature rise of ~10 to 15°F was measured on the transducer mounting plate surface after one run. It is not clear whether this 'anti-icing' was simply a heating effect or due to the ultrasonic vibration of the surface or some combination of both. However, it served as a useful de-icer in these tests.

On the night of 18 December, LWC was increased to 1.35 $g/m^3$, while maintaining the slow 50 mph flow speed. For Set 2, tunnel temperature was set at 0°F. The first run (2-1) was with the acoustic power OFF, providing unperturbed ice accretion thicknesses. Runs 2-2 to 2-4 sequentially powered the different pairs of the ultrasonic transducers and different driving frequencies in the tweeters. Run 2-5 again was a transducer OFF run. The unexpectedly low ice accretion for Run 2-1 in Figure 13 was the first run of the night and was attributed to unequilibrated tunnel operating conditions.

The variation between Runs 2-1 and 2-5 emphasized the importance of running as many OFF as ON experiments in order to measure variability of ice accretion under 'constant' icing conditions. This was particularly important in view of the negative results, i.e. it was necessary to establish how small an anti-icing effect could be detected.

For Set 3 the tunnel was cooled to -30°F. Run 3-1 was again a null run. Starting with Run 3-2 and then with 3-4 and 3-5, the ultrasonic transducer and tweeter frequencies were again sequentially powered. Since ice accretion during Run 3-2 was so much deeper than that in 3-1, another OFF run (3-3) was immediately taken which showed that Run 3-1 was anomalous. At that time, it became clear that, due to a temperature programming error in the IRT control software, that Run 3-1 has actually been about 2°F colder than the -30°F target temperature. The shallow ice accretion observed at -32°F was the first indication of spontaneous freezing

of the droplets in the wind tunnel as tunnel temperatures neared the homogeneous freezing point of pure water (-40°F).

This was readily apparent when the tunnel was cooled to -36°F in Run 4 as displayed in Figure 14. Ice accretion thickness decreased sharply (to ~ 0.1" average thickness), presumably reflecting the degree of spontaneous freezing of the droplets in the tunnel, independent of any added perturbations. Due to lack of tunnel time at the end of the evening, only three runs could be recorded, two OFF (4-1 and 4-3) with one ON (4-2). There was significant variability in the observed ice accretion thicknesses; the degree of spontaneous freezing is very sensitive to the precise operating conditions of the tunnel. Looking at the relative thicknesses in Figure 14, there is no indication of a (statistically) significant reduction in ice accretion for the transducer ON Run 4-2.

### 3.3 Summary

The ice accretion/acoustic transducer testing apparatus performed very much as planned. The IRT facility operated nearly flawlessly. During the first day (16 December) all problems concerning assembly and integration of the transducers and flow duct were resolved. Furthermore, integration of the computer control system and the tunnel control room facilities went very smoothly. NASA provided an IBM compatible PC to speed up software control of transducer drive frequencies. During actual testing, NASA personnel were able to provide exactly the super-cooled cloud conditions requested.

The flow duct/airfoil design provided well-defined ice accretion conditions. Ice thicknesses on the order of 0.5" in 10 minutes of tunnel time were ideal for anti-icing testing. The ice profiles were uniform (for the most part) and reproducible. The profiles do show some asymmetry which appears to be a property of the duct itself, uncorrelated with transducer operation. The fall-off of icing at the edges is consistent with expected boundary layer effects. Overall, it appears that the flow duct served its purpose of providing a reproducible well-defined center line flow, as demonstrated by similar accretions on the downstream airfoil.

The transducer assembly also performed as designed, though it was apparent that, in the case of the ultrasonic transducers, higher power levels could be achieved with better impedance matching and more electronic amplification. The problem was the lower operating temperature and increased cooling in IRT. The lower temperatures shifted the resonant frequencies of the transducers, invalidating much of the impedance matching/resonance calibration testing performed at ARI the week before at room temperature. Furthermore, in the wind tunnel flow it became clear that the transducers could be powered beyond the capacity of the ENI amplifier.

As summarized in Figure 15, the overall result of the testing is that the ice measurements show no evidence of any reduction of accretion by the acoustic power. Over a wide range of tunnel conditions (e.g. temperature, speed and LWC), there is no statistically significant difference in ice accretion due to the presence of ultrasonic energy. The desired reduction in ice accretion simply was not observed. Beyond the ice thickness measurements plotted in Figures 12-15, direct examination of the accreted ice showed no indication of any changes in ice morphology with the acoustic power ON.

The variation in ice accretion thickness is seen most clearly in Figure 16, which plots ice thickness versus temperature. Ice accretion thickness has been normalized to the liquid water content (LWC) in the IRT. The normalization places data from Set 1 on the same relative scale as Sets 2-4. This normalization is not rigorous, since one should also include the collection efficiency whose estimation would requires detailed air flow calculations. This would have the largest effect on Set 1 (at -20°F) whose smaller droplet size (14 versus 40 μm MVD; see Table 2) would reduce the collection efficiency. Thus, the plot in Figure 16 probably underestimates the relative ice accretion thickness at -20°F.

Figure 16 indicates that ice accretion on the streamline airfoil peaks at about -20°F, perhaps reflecting a maximum in sticking probability for droplets supercooled at that temperature. More importantly, below -20°F ice accretion drops off, especially below -30°F where it drops sharply. This is exactly what one expects as the homogeneous freezing point is approached (for example, see reference 1). This sharp drop off clearly explains the shallow ice accretion observed in Run 3-1, when the IRT temperature was not being properly regulated. The plot in Figure 16 implies that the tunnel temperature may actually have been lower than the -31.9°F that was extracted from the ESCORT thermocouple readout printed at the end of the run. Unlike every other run, regulation/monitoring of temperature by IRT operators was unreliable during Run 3-1 due to a programming error which was detected between Runs 3-1 and 3-2.

Most importantly the conditions for Set 3 and 4 were optimal for observation of an acoustically-induced ice nucleation effect. The low ice accretion is evidence of the desired anti-icing effect: droplets that freeze before impinging on the airfoil bounce rather than stick. The temperature scale of Figure 16 is very consistent with fundamental cloud microphysics. The sharp ice fall-off with temperature indicates that the remaining unfrozen supercooled droplets are just below threshold for ice nucleation. That is the most sensitive point at which to observe a perturbation of ice nucleation probability. Thus, the lack of any indication of an acoustically-induced ice accretion reduction represents a clear negative result.

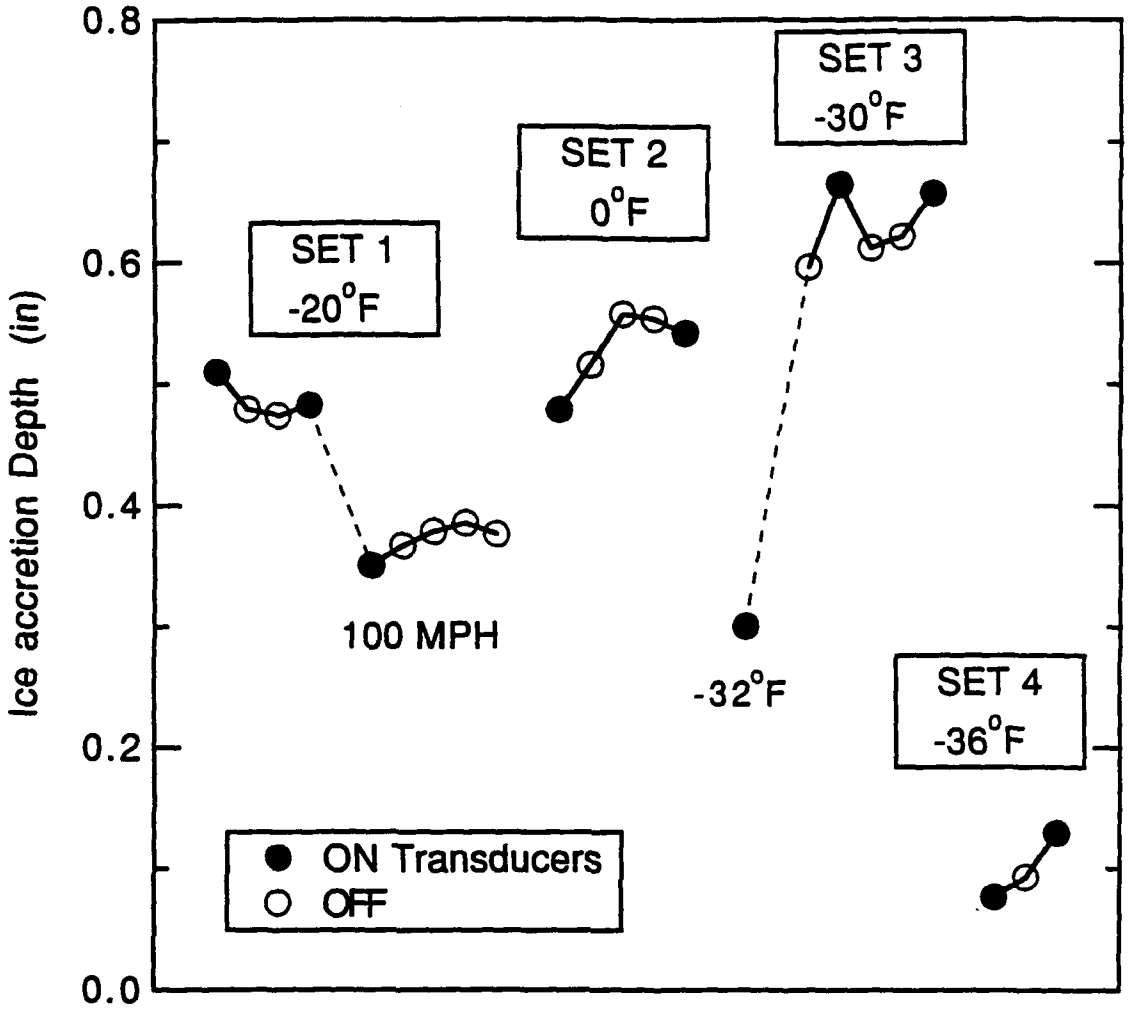


Figure 15. AVERAGE ICE ACCRETION THICKNESSES FOR THE CENTRAL AIRFOIL SPAN

The ice accretion in the central region of the airfoil away from the depleted edges is averaged for all runs in each of the data sets and is plotted in the order the data were taken.

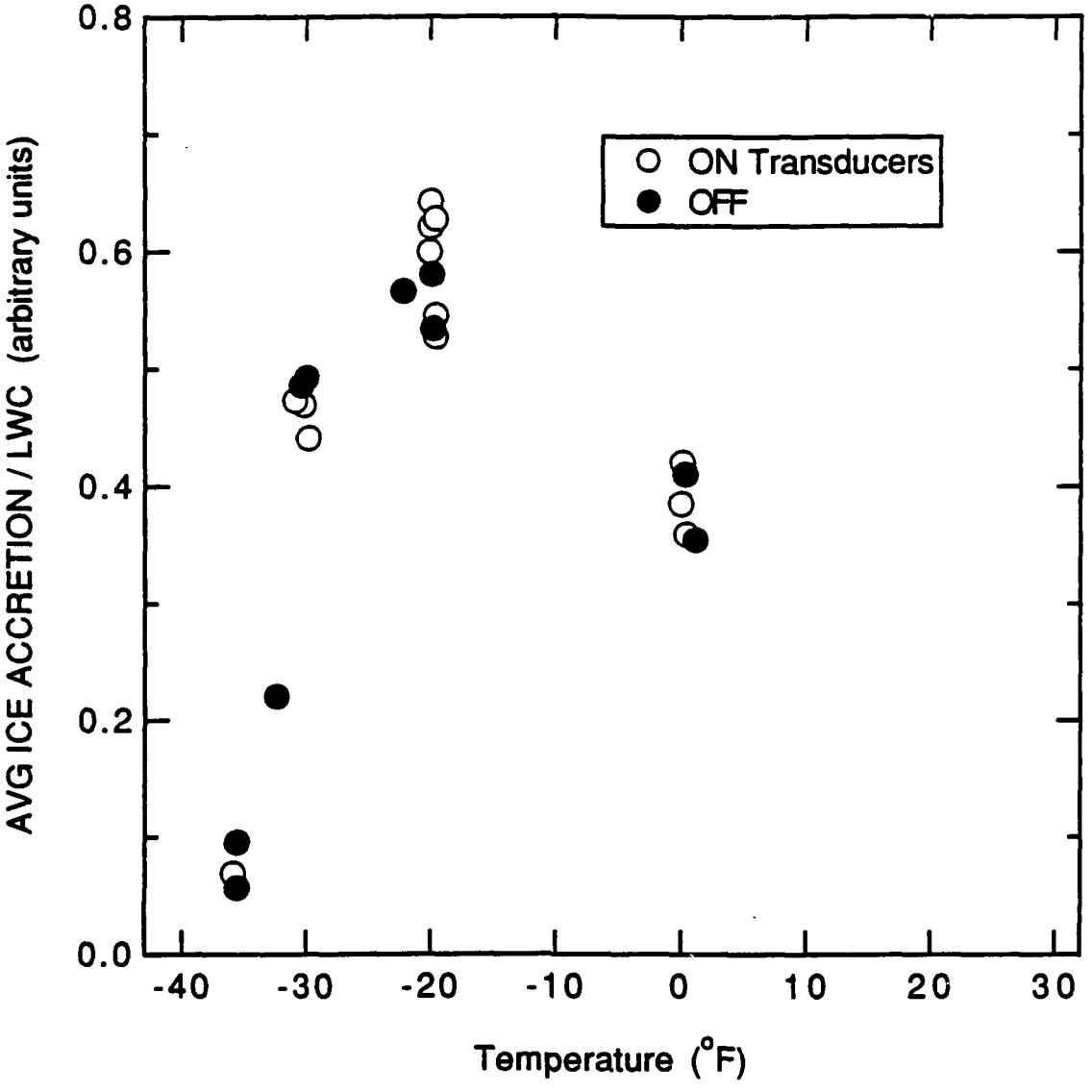


Figure 16. NORMALIZED ICE ACCRETION THICKNESSES
The data in Fig. 15 are divided by the liquid water content corresponding to the individual run and plotted versus tunnel temperature. It is apparent that spontaneous freezing is reducing the normalized ice accretion thickness in the range of -25 to -36°F and that the transducers do not have any effect above the experimental uncertainty. As discussed in the text, the normalized thickness for the Set 1 data at -20 F probably underestimate the relative ice thickness.

Comparison of the conditions explored in Table 2 with the test plan shown in Figure 11 shows that the tests followed the plan on the negative effects (left) side of the diagram. The one flaw in the overall test procedure was the use of high (1.35 $g/m^3$) LWC in the tests at the coldest temperatures on the night of 18 December. Unfortunately ARI personnel did not realize at the time that this high LWC had nearly tripled the average droplet size (40 $\mu$m versus 14 $\mu$m MVD at lower LWC). This is significant in view of the freezing times listed in Table 1. Realizing that $t_f$ scales as the diameter squared, for 40 $\mu$m droplets at -30°F the predicted freezing distance at 50 mph is 1.2 meter. While this is shorter than the 2 meter distance actually between the irradiated volume and the airfoil in the flow duct, expected results for the initial tests were to observe the smallest droplets possible to maximize freezing rates. For that reason and in view of the negative results, the transducers were not moved forward to check shorter freezing times.

As mentioned above, no further tests were undertaken after 18 December. Optimal supercooled conditions had been tested and the negative results did not indicate that further testing could be justified as a productive use of NASA IRT resources.

# 4. DISCUSSION

The goal of this research project was to demonstrate that acoustically induced nucleation of supercooled water droplets can result in freezing the droplets. To this end, a total of nine acoustic transducers were specified, mounted and coupled to specially designed flow duct and airfoil, which were placed in the center of the NASA LeRC IRT facility. The design, assembly and integration of this apparatus, done collaboratively with NASA and ARI personnel, was accomplished almost exactly according to plan. The operation of the transducers and the IRT during testing went well. Unfortunately, no acoustically induced effects on ice accretion were observed.

In the remainder of this section, the results in terms of their implications for ice nucleation (and icing prevention) and of possible reasons for the negative effects are discussed. This includes possibilities for improving and extending the experimental program. ARI concludes with a summary of conclusions and recommendations.

## 4.1 Ice Accretion Observations

The ice accretion profiles (Figs. 12-14) measured for various cloud conditions and temperatures were seen to depend on the tunnel parameters. The maximum ice thickness along the airfoil span varied from about 0.1 inch to about 0.6 inch as the temperature, droplet size, and liquid water content were changed. The ice accretion thickness also varied along the span, dropping to smaller values near both ends and sometimes having a definite asymmetry end-to-end. The end-to-end asymmetries do not correlate with transducer operations nor with mean tunnel conditions: temperatures and cloud conditions. The most likely source for such variations are local non-uniformities in the liquid water content of the spray cloud, whether due to the tunnel as a whole or due to perturbations caused by introducing the flow duct in the test section. The greatest measured asymmetries are larger than expected from the reported LWC uniformity profiles in the IRT Users Manual (Ref. 10) although, for other runs, very good uniformity was observed.

The reduced and integrated profiles (Fig. 15), representing the total accreted ice away from boundary layer effects, demonstrates that all of the variation in ice thickness is attributable to tunnel conditions. The decrease in ice thickness at the ends of the span are due to droplets depositing on the internal flow duct walls as the sampled flow convects toward the airfoil. Deposits on the internal walls were observed and required cleaning where they might impact the transducer operation. It is interesting to note that, when any of the transducers or tweeters were operating at high power levels, their emitting surface did not accrete ice (except for the 350 kHz, which always accreted at least some ice). Given the modest

temperature rises on their emitting surfaces, this effect seems to be due to solid acoustic wave motion interfering with the ice accretion process.

The only variations remaining after normalizing by the cloud liquid water content (see Figure 16) is a systematic variation with temperature and run-to-run variation that cannot be correlated systematically with transducer parameters. The temperature dependence shows an increasing normalized ice accretion as the temperature decreases until spontaneous freezing begins below -20°F. Ice accretion is nearly totally suppressed due to spontaneous freezing at -36°F. The run-to-run variation does not correlate with transducer frequencies being used and appears to be wholly due to experimental uncertainties, either in tunnel conditions or measurement errors. These results indicate that, over the range of frequencies and power levels used to excite the super-cooled droplets, acoustic suppression of ice accretion does not occur. The ice accretion measurement used is sensitive to complete and partial freezing of the droplet cloud as is evidenced by the drop in ice accretion as spontaneous freezing progresses. Various degrees of cloud freezing resulted in the decreasing ice thickness as spontaneous freezing progresses into the -25°F to -35°F range.

If acoustically induced nucleation had occurred, partial freezing would have happened almost instantaneously and continued until the droplet temperature rose to the freezing point. The only way that nucleation could have happened and not resulted in a measurable difference in ice thickness would be if ice accretion was not affected at all until the droplet was completely frozen. In order for this situation to have occurred in the present experiments, the evaporative cooling rates for the droplets calculated (See Table 1 in Section 1) would have to be in error by almost an order of magnitude. For these reasons, it is believed that no nucleation was induced with the ultrasonic levels employed in these experiments.

## 4.2 Acoustic Power Levels

The total acoustic power within the excitation volume depends on he power delivered to the transducer and its coupling to the acoustic radiation field that leaves the transducer surface. The single-frequency transducer manufacturer and the tweeter supplier both provided specifications for optimizing the coupling efficiency. The single-frequency transducers are impedance matched with air in a quarter-wave coating on their active surface. Acoustic coupling was measured for all the transducers used in this study and was found to be consistent with the manufacturers' specifications. While these couplings are considered quite high for the coupling of solid-acoustic waves into air and for audio equipment, only a small fraction of the total power supplied to the transducers actually propagates into the duct.

The acoustic coupling losses for each of the transducers are listed in Table 3, along with the sound pressure level (SPL) in dB for a representative input power level. The lower tweeter frequencies combined with the smaller tweeter acoustic aperture result in significantly more diffraction of the energy for these cases. The table entry for the tweeters is for the SPL at the center of the duct, with higher levels near the aperture and lower levels further away. The higher piezoelectric frequencies do not diffract significantly for their transducer sizes and wavelengths.

Reflections, which may make local levels higher and may also introduce standing waves and nodal patterns, are not included in these estimates.

Table 3. Acoustic Power Levels

| Frequency (kHz) | Coupling Losses(dB) | Input Power(W) | SPL(dB) at 30 cm |
|---|---|---|---|
| 20-40 | 32-35 | 15 | 115 |
| 80 | 35 | 50 | 125 |
| 340 | 35 | 50 | 125 |
| 650 | 35 | 50 | 125 |

By increasing the coupling efficiency further, more acoustic power would be available to excite the super-cooled droplets in the flow more strongly . Increases in coupling efficiency could raise the acoustic power levels by from two to over three orders of magnitude (recovering 20 to 35 dB coupling losses of the various transducers). For any realistic impedance matching, residual losses will prevent complete recovery of all the coupling losses, but substantial improvements beyond the performance of the current transducer set is considered possible by the manufacturer (NUTRAN).

## 4.3 Operating Parameters

The existing empirical evidence for acoustically induced freezing has all been obtained in natural clouds or in cloud chambers where freezing times are not limited. The effective freezing times in the present experiments, for 50 mph (22 m/s) tunnel speed and less than 2.4 m between the transducers and the airfoil, all are below about 0.1 sec. It is conceivable that crystallization nucleation had begun even in the experiments reported here, but in this flow system, there had not been sufficient time for the crystallization to propagate throughout the individual droplets. If the heat of

fusion cannot be removed from the freezing droplets quickly enough, as described previously, completion of droplet freezing will become kinetically limited.

An alternative means of exploring the detailed mechanism responsible for the previously observed freezing would make use of a cloud chamber to repeat the conditions of these earlier experiments. Power thresholds, frequency dependencies, and the temporal behavior of the freezing process could then be measured quantitatively and experimental conditions for a successful icing wind tunnel study could be calculated. Cloud chamber facilities at Cold Regions Research and Engineering Labs in Hanover, New Hampshire and at the Colorado State University at Fort Collins (See Reference 1) have been canvassed and both have facilities where such studies could be performed.

While no previous experiments have quantified the power levels or frequency dependence of those empirical observations, the van Stratten-Allen patent[6] refers to super-audible frequencies (they quote the range of 15-30 kHz) at power levels above 150 dB. Their patent grew out of cloud chamber work where freezing times were not limited by flow times. They do not provide evidence that 150 dB is a SPL threshold for acoustically inducing droplet freezing. Verbal communication with F. van Straten indicates that the threshold SPL level was not measured in any detailed way, but it is worth noting that the SPL levels used in the present experiments are 25-35 dB lower than this value.

While the means of increasing SPL levels in the high frequency range (above 80 kHZ) is probably best accomplished with improvements in the impedance matching of the piezoelectric transducers, an alternative transducer may be required to increase the SPL in the tweeters' frequency range. The van Straten-Van Allen patent proposes using a siren operating in the 15-30 kHz range at a SPL of 150 dB and electronic sirens are available commercially that roughly correspond to their suggested acoustic driver.

At this point, it should be noted that simple utilization of such a commercial siren (or increased transducer amplifier capability) probably would not be practical in actual icing prevention systems. A 30 kHz operating frequency may be too close to the audible and power requirements may be excessive. The key point is that, given positive ice freezing results, observed under any conditions, there will be ample room for engineering improvements to design and construct a realistic device.

### 4.4 Summary

The basic conclusion to be drawn from these anti-icing tests is that, for the range of ultrasonic power levels (~125 dB) and frequencies (20kHz to 650 kHz) used with the flow times (~100 ms) provided for droplet freezing, no measurable effects on ice

accretion were observed. The tunnel temperature was varied, including temperatures low enough (-36°F) for spontaneous freezing to occur independent of the ultrasonic excitation, and the temperature dependence of ice accretion was observed. Particularly at the lowest temperatures, ultrasonic induction of freezing was expected to affect ice accretion if the operational parameters were above the threshold for nucleation.

Given that anecdotal evidence does exist for acoustic (both audible and ultrasonic) induction of freezing, it appears that the current experiments do not have a large enough operating envelope to capture the relevant processes. It is important to note that the present results report quantitative experimental conditions for acoustic excitation of cloud droplets for the first time. They provide a set of baseline conditions for any further exploration of the parameter space of acoustic power, excitation frequency, and freezing time for these type of cloud conditions. The induction of freezing appears to be a threshold phenomenon, and is undoubtedably highly nonlinear in any case.

Expansion of the parameter space (or operating envelope) in any future experiments should be focussed on 1) increasing transducer power and 2) increasing the freezing time. While frequencies could also be varied further into the audible range and further into the ultrasonic range, the broad range used in the present studies extends from where attenuation in air becomes important at the short wavelengths up to several millimeters, much larger than the droplet sizes. The transmitted transducer powers were below the referenced power level of 150 dB in the van Straten-van Allen patent. These levels could be increased by engineering improvements in the transducer designs and/or an alternate acoustic source could be considered. Commercially available electronic sirens have specifications to higher power levels than used in the present study and their use in future experiments would be recommended if appropriate frequency response could be obtained.

The addition of a second ENI high frequency amplifier would double the available ultrasonic transducer power. It would also enable separate frequency tuning and impedance matching of each ultrasonic transducer pair. This, together with the siren mentioned above, would do much to close the gap between the current 125 dB power level and the 150 dB level specified by Van Straten.

Greatly increased freezing times are not possible in the NASA LeRC IRT. The tunnel was running at the lower end of its speed range and the flow duct could not be extended significantly without having the boundary layers affect most of the flow cross section. The most feasible means of increasing the freezing time would be to perform similar experiments statically in a stationary cloud. Several possible laboratory facilities exist for such experiments.

# 5. Conclusions

1. No changes in ice accretion rates (i.e., no icing prevention) due to acoustic perturbation were observed.

2. Acoustic power levels (up to 125 Db) were about as high as planned. However, future enhancements (better impedance matching, increased power amplification) are possible based on IRT experiments.

3. Failure to observe icing reduction may reflect non-linearity of ice nucleation process; experimental parameters may still lie below operational envelop (nucleation threshold).

4. Convection times in the icing tunnel may not have been long enough to provide sufficient droplet freezing.

5. This series of tests provides the first systematic baseline for evaluating anecdotal evidence of acoustically induced nucleation.

6. The anecdotal observations of acoustically-induced nucleation should be understood systematically by expanding the frequency/power/freezing time operational envelope.

7. It is important to note that, once that the operational envelope is characterized, ultimate feasibility of aircraft icing prevention may depend on engineering development in transducer design.

## 6. REFERENCES


1. DeMott, P.J. and Rogers, D.C. (1990) "Freezing Nucleation Rates of Dilute Solution Droplets Measured Between -30° and -40°C in laboratory Simulations of Natural Cloud," J. of Atmos. Sci. 47, 1056-1064.

2. B.J. Mason, "Clouds, Rain and Rain Making," p. 69, Cambridge University Press (1975).

3. S.S. Hirano, "Ecology and Physiology of Pseudomonas Syringae," Bio. Tech, 3, 1073 (1985).

4. R.L. Ives, "Detection of Supercooled Fog Droplets," J. Aeron. Sci., p 120 (1941).

5. W.C. Swinbank, "Crystallization of Supercooled Water by Ultrasonic Radiation", J. of Meteoro., 14, 190 (1957).

6. F.W. Van Straten and W.A. Van Allen, "Method of Crystallizing Supercooled Water Droplets",U.S. Patent No. 2,480,275 (1949).

7. D.R. Worsnop and Z. Hed, "Development of Icing Prevention by Nucleation of Ice Particles in Front of Subsonic Aircraft", Final Report, ARI-RR-858, DOT Contract No. DTRS-57-90-C-00132 (1991).

8. M.S. Zahniser, D.R. Worsnop, C.E. Kolb, J.M. Van Doren, L. Watson and P. Davidovits, "Heterogeneous Reaction Kinetics of Importance to Stratospheric Chemistry", Final Report, ARI-RR-674, Chemical Manufacturers Association, Contract No. 87-653 (1988).

9. D.R. Worsnop, M.S. Zahniser, C.E. Kolb, J.A. Gardner, L.R. Watson, J.M. Van Doren, J.T. Jayne and P. Davidovits, "Temperature Dependence of Mass Accommodation of $SO_2$ and $H_2O_2$ on Aqueous Surfaces," J. Phys. Chem.93, 1159-1172 (1989).

10. Soeder, R.H. and Andracchio, C.R. "NASA Lewis Icing Research Tunnel User Manual", NASA Technical Memorandum 102319 (1990).

# APPENDIX A

## METHOD OF CRYSTALLIZING SUPERCOOLED WATER DROPLETS

F.W. Van Straten and W.A. Van Allen
U.S. Patent No. 2,480,275
1949

Patented Aug. 30, 1949

2,480,275

# UNITED STATES PATENT OFFICE

2,480,275

## METHOD OF CRYSTALLIZING SUPER-COOLED WATER DROPLETS

Florence W. van Straten, Green Acres, Md., and William A. Van Allen, Boston, Mass.; said Van Allen assignor to said van Straten

No Drawing. Application October 4, 1947, Serial No. 778,020

4 Claims. (Cl. 244—134)

1

Our invention relates to meteorology and comprises a method of crystallizing super-cooled water droplets lying in the path of an airplane in order to prevent the formation of ice thereon.

The most important object of our invention is to improve the safety with which aircraft operations may be conducted.

Another object of the invention is to increase the military efficiency of aircraft, particularly in frigid regions.

A further object of the invention is to provide practical compact means to be carried by a plane and useful to eliminate the hazard of ice formation on wings and other exposed surfaces.

Although some of the meteorological phenomena involved are not too clearly understood, it is known that the atmosphere may contain, in certain zones, water droplets in a metastable, super-cooled condition at temperatures as low as —35.0° C. It has been shown experimentally that ice crystals and super-cooled water droplets may exist simultaneously in clouds where the upward component of air velocity is sufficient to effect the production of super-cooled droplets faster than they can evaporate over to nearly ice crystals.

Some crystallization of the droplets is brought about as the result of collisions due to Brownian movement of the droplets: the crystallization takes place on dust motes or other nuclei present in the cloud. The rate at which such random crystallization occurs is closely dependent on temperature. For example the rate at —35.2° C. is $10^{12}$ as great as at —34.8° C. If the temperature falls significantly below —35.0° C., substantially all of the droplets will crystallize.

Moreover, if a super-cooled droplet is subjected to distorting stresses as by in intense sound wave or by impact on a moving surface, its metastable condition of equilibrium is disturbed, and it turns almost at once to ice. This is the manner in which ice forms on aircraft wings and the like.

Heretofore the problem of eliminating ice formation on aircraft has been directed along three avenues of attack. One system comprises employing resilient boots for protection of vital surfaces: after ice forms on the boots, the pilot flexes them to crack off the ice. Another method is to conduct a hot fluid to the vicinity of the surface to be protected in order to melt the ice as it forms. Chemical compounds have been applied to such surfaces in order to reduce their adhesive qualities and thereby inhibit ice formation. However, no one thus far has produced a completely satisfactory solution to the problem.

2

We have discovered that sound waves of proper frequency and intensity may be focused in a beam and used to produce almost instantaneous crystallization of super-cooled water droplets. By mounting a suitable sonic generator and radiator, or horn, upon a plane, we can project a sound beam ahead of the plane and crystallize the super-cooled droplets lying ahead of it. The ice crystals then either bounce off the plane or flow by it in the air stream. Consequently ice does not build up on any of the surfaces thereof.

We believe that the effect of sound waves on the super-cooled droplets is two-fold. Accompanying the sound waves is an adiabatic temperature change; at 150 db. R. M. S. pressure level this change is .05° C., but at 160 db. the change is 1.88° C. Consequently the sudden temperature drop may, in certain cases, act to increase random crystallization to the point where substantially all of the droplets in the immediate vicinity will rapidly crystallize.

Furthermore the pressure gradient accompanying the progressive sound waves brings distorting stresses to bear on the droplets, again disturbing their condition of equilibrium and effecting almost instantaneous crystallization thereof.

Inasmuch as the propellers of a plane emit a considerable volume of sound at various frequencies without affecting the formation of ice, it is obvious that sound per se is not sufficient and that frequency and intensity must be carefully selected if the desired results are to be obtained on a satisfactory scale.

To make full use of the pressure wave aspect of the sound waves the frequency must be such that there will be definite motion of the air with respect to the droplets. Below 1 kc. the droplets will move with the air with almost no relative movement between individual drops. Above 30 kc. the attenuation of sound energy is great, and the necessary intensity must be maintained a sufficient distance ahead of the plane to give the droplets time to crystallize before being struck by the plane. Consequently, 30 kc. would appear to be a preferable upper limit of frequency. However, since the desired effects may be obtained at frequencies up to 100 kc., the scope of our invention is not limited to 30 kc. as an upper limit.

Inasmuch as sound is more easily focused as its frequency increases and since a beam is desired in order to concentrate the available energy in the most useful areas, we find that a frequency of from 15 to 30 kc. is preferable. Incidentally, one advantage of this range is that

it lies above the audible limit. Consequently an installation of equipment for performing the method of the invention does not constitute a nuisance from the standpoint of noise.

While the apparatus used forms no part per se of our invention, we suggest the use of a powerful siren capable of producing sound at an intensity of better than 150 db. and at a frequency in the range 15–30 kc. The siren may be coupled to a radiating horn serving to focus the sound from the siren into a fan-shaped beam. By mounting the horn at a central point on the plane, we are able to project a sonic beam along the natural direction of movement of the plane and thereby effect crystallization of super-cooled water droplets lying in its path. The beam is so radiated as to effect crystallization through an area lying sufficiently far ahead of the plane to permit complete crystallization and broad enough to extend completely across the width of the plane.

Having thus disclosed our invention, what we claim as new and desire to secure by Letters Patent of the United States is:

1. A method for preventing ice formation on moving surfaces, comprising crystallizing supercooled water droplets lying in the path of flight by projecting a sound beam ahead of the moving surface and through a cross-sectional area at least as wide as said surface, said sound beam comprising sound waves at a frequency of 15 kc.–30 kc. and an intensity of greater than 150 decibels, which frequency and intensity will be sufficient to cause vibration which imparts sufficient distortional stresses within the droplets to crystallize the same.

2. A method for crystallizing super-cooled water droplets suspended in air, comprising subjecting the droplets and surrounding air to the action of sound waves having an intensity of at least 150 db. and at a frequency of from one to one hundred kilocycles, which frequency and intensity will be sufficient to cause vibration which imparts sufficient distortional stresses within the droplets to crystallize the same.



3. A method for crystallizing super-cooled water droplets suspended in air, comprising subjecting the droplets and surrounding air to the action of sound waves having an intensity of at least 150 db. and at a frequency above the audible limit but less than 100 kc., which frequency and intensity will be sufficient to cause vibration which imparts sufficient distortional stresses within the droplets to crystallize the same.

4. A method of protecting a moving surface against ice formation, comprising crystallizing super-cooled water droplets lying in the path of movement by projecting a sound beam ahead of and in the direction of travel of the surface, the sound beam comprising sound waves at a frequency between 15 and 100 kc. at an intensity of at least 150 db., which frequency and intensity will be sufficient to cause vibration which imparts sufficient distortional stresses within the droplets to crystallize the same.

FLORENCE W. VAN STRATEN.
WILLIAM A. VAN ALLEN.


REFERENCES CITED

The following references are of record in the file of this patent:

UNITED STATES PATENTS

| Number | Name | Date |
|---|---|---|
| 1,980,171 | Amy | Nov. 13, 1934 |

# APPENDIX B

## ESTIMATE OF POWER REQUIREMENTS FOR ULTRASONICALLY INDUCED ICE NUCLEATION

## APPENDIX B: ESTIMATE OF POWER REQUIREMENTS FOR ULTRASONICALLY INDUCED NUCLEATION

Energetics of ice nucleation involve consideration of the surface energy of embryonic nuclei, about which little is known. In one limit, the surface energy density ($E_s$) required to form an embryonic nucleus (of radius r) can be approximated by the heat of fusion ($C_f$) of its volume, which gives an energy density of

$$E_s = 10^{-3} \text{ joule/cm}^2$$

This formulation estimates that the energy barrier to formation of an ice-like surface within liquid water is equal to the energy gain in forming an ice crystal. This is not an unreasonable assumption for molecular rearrangement processes; it probably gives an upper limit to the barrier. The actual magnitude of the barrier depends on the detailed mechanism of the water/ice transition.

Another approach to estimating surface energy is to consider the energy required for bubble formation. In other words, consider the ultrasonically induced ice formation as a cavitation nucleation process. For small droplets (for which the heat of vaporization of the interior volume is negligible), the surface energy density is simply given by the surface tension of water:

$$E_s = 75 \text{ dyne/cm} \sim 10^{-5} \text{ joule/cm}^2$$

This smaller value clearly indicates that water surfaces can be perturbed by energy densities far lower than the upper limit stated above. Although not convinced that bubble formation is required for ice nucleation, ARI will use this energy density estimate as a more realistic estimate of the energetics of liquid perturbations.

The next question is the time in which this surface energy needs to be delivered to the droplet. In other words, what is the power density required to produce embryonic nuclei for ice crystallization? This can be estimated by considering nucleus formation as a molecular rearrangement process, whose rate can be estimated by the rate of molecular diffusion within the liquid. Then, the time scale is given by

$$t = r^2/D_l$$

where $D_l$ is the diffusion coefficient of water. For $D_l = 10^{-5}$ cm$^2$/s and $r = 10^{-5}$ cm, one obtains

$$t = 10^{-5} \text{ s}$$

Combining this with $E_s$ above, a required power density of $E_s/t \sim 1$ watt/cm$^2$ is obtained.

In order to compare this power with that of the transducer, one needs to know the coupling efficiency of the transducer power. As described in the proposal resulting in this study, that efficiency can be approximated from the acoustic impedances of air and water ($R_A$ and $R_W$), whose ratio ($R_A/R_W$) is about $3x10^{-4}$. The exact expression for acoustic energy transfer, expressed as the transfer coefficient ($\alpha_T$) is

$$\alpha_T = 4R_AR_W/(R_A + R_W)^2$$

In the limit of $R_A >> R_W$, which is true here,

$$\alpha_T = 4R_W/R_A$$

which gives air/water acoustic coupling of $\sim 10^{-3}$. Combining this efficiency with a 10 watt/cm$^2$ transducer, one estimates a power density of $\sim 10^{-2}$ watt/cm$^2$. This clearly is much lower than the requirement of 1 watt/cm$^2$ estimated above.

There is considerable uncertainty in this estimate for the required power density. For example, assumption of $r = 10^{-5}$ cm is critical to the final results. The purpose of the calculation was to give a rough picture of nucleation energetics. It is interesting to note that this 1 watt/cm$^2$ power level (in the context of Table 3 in Section 4) is not inconsistent with the 150 dB threshold power level quoted in the van Stratten patent.[6]

The acoustic power level can also be considered as pressure perturbation ($\Delta P$), e.g. 150 dB in air corresponds to ~630 Pascal. This can be compared to the surface tension of water ($E_S$) by assuming a particle radius (r), i.e.

$$\Delta P \sim E_S / r$$

This gives r~115 $\mu$m. For the droplet size range of interest (5-30 $\mu$m diameter) about an order of magnitude more power is required for perturbing the surface of the entire droplet, e.g. a power level of ~ 170dB.

The first estimate of 1 watt/cm$^2$ considered the energetics and dynamics of perturbing a small crystallization nucleus as opposed to the whole droplet. The two estimates show the uncertainties in predicting the required power levels in the absence of detailed understanding of the microphysics. The point is that the threshold character of the nucleation process makes the acoustic power level critical to observation of positive effects.